

Research Article

Use of the Polo-like kinase 4 (PLK4) inhibitor centrinone to investigate intracellular signalling networks using SILAC-based phosphoproteomics

Dominic P. Byrne^{1,*}, Christopher J. Clarke^{1,2,*}, Philip J. Brownridge², Anton Kalyuzhnyy^{1,3}, Simon Perkins^{1,3}, Amy Campbell^{1,2}, David Mason⁴, Andrew R. Jones^{1,3},  Patrick A. Evers¹ and  Claire E. Evers^{1,2}

¹Department of Biochemistry and Systems Biology, Institute of Systems, Molecular and Integrative Biology, University of Liverpool, Liverpool L69 7ZB, U.K.; ²Centre for Proteome Research, Department of Biochemistry and Systems Biology, Institute of Systems, Molecular and Integrative Biology, University of Liverpool, Liverpool L69 7ZB, U.K.;

³Computational Biology Facility, Department of Biochemistry and Systems Biology, Institute of Systems, Molecular and Integrative Biology, University of Liverpool, Liverpool L69 7ZB, U.K.; ⁴Department of Biochemistry and Systems Biology, Centre for Cell Imaging, Institute of Systems, Molecular & Integrative Biology, University of Liverpool, Liverpool L69 7ZB, U.K.

Correspondence: Claire E. Evers (ceyers@liverpool.ac.uk) and Patrick A. Evers (Patrick.evers@liverpool.ac.uk)



Polo-like kinase 4 (PLK4) is the master regulator of centriole duplication in metazoan organisms. Catalytic activity and protein turnover of PLK4 are tightly coupled in human cells, since changes in PLK4 concentration and catalysis have profound effects on centriole duplication and supernumerary centrosomes, which are associated with aneuploidy and cancer. Recently, PLK4 has been targeted with a variety of small molecule kinase inhibitors exemplified by centrinone, which rapidly induces inhibitory effects on PLK4 and leads to on-target centrosome depletion. Despite this, relatively few PLK4 substrates have been identified unequivocally in human cells, and PLK4 signalling outside centriolar networks remains poorly characterised. We report an unbiased mass spectrometry (MS)-based quantitative analysis of cellular protein phosphorylation in stable PLK4-expressing U2OS human cells exposed to centrinone. PLK4 phosphorylation was itself sensitive to brief exposure to the compound, resulting in PLK4 stabilisation. Analysing asynchronous cell populations, we report hundreds of centrinone-regulated cellular phosphoproteins, including centrosomal and cell cycle proteins and a variety of likely ‘non-canonical’ substrates. Surprisingly, sequence interrogation of ~300 significantly down-regulated phosphoproteins reveals an extensive network of centrinone-sensitive [Ser/Thr]Pro phosphorylation sequence motifs, which based on our analysis might be either direct or indirect targets of PLK4. In addition, we confirm that NMYC and PTPN12 are PLK4 substrates, both *in vitro* and in human cells. Our findings suggest that PLK4 catalytic output directly controls the phosphorylation of a diverse set of cellular proteins, including Pro-directed targets that are likely to be important in PLK4-mediated cell signalling.

Introduction

Polo-like kinases (PLKs) are key cell cycle Ser/Thr kinases conserved in metazoan organisms. Four kinase-domain-containing PLK family members are found in most kinomes, and each PLK polypeptide is thought to serve specific functions in cells. Polo-like kinase 4 (PLK4) is the central regulator of centriole assembly [1,2]. Specifically, PLK4 activity is rate-limiting for centriole duplication, a process that requires hierarchical recruitment of many evolutionarily conserved core proteins: PLK4/SAK/STK18/ZYG-1 itself, SAS-5/Ana2/STIL, SPD-2/DSpd-2/CEP192, Sas6 and Sas4/CPAP to a single assembly site on the mother centriole [3], driven by its role in phosphorylating key components of the centriolar duplication machinery, notably STIL. Overexpression of PLK4 induces centrosome amplification from pre-existing centrioles and drives *de novo* centriole assembly [1–8]. In human cells, PLK4

*Equal contribution.

Received: 21 April 2020
 Revised: 27 May 2020
 Accepted: 5 June 2020

Accepted Manuscript online:
 5 June 2020
 Version of Record published:
 2 July 2020

is recruited to the centriole during G1 phase through interaction with CEP152 and CEP192. At the G1/S transition, PLK4 transforms from a ring-like localisation to a single focus on the wall of the parent centriole that marks the site of procentriole formation [9–12]. Binding of PLK4 to the physiological centriolar substrate STIL promotes activation of PLK4, and the subsequent binding and recruitment of SAS6 [13–16].

Distinct from its canonical rate-limiting role in the control of centriolar duplication, non-centriolar PLK4 has also been implicated in actin-dependent cancer cell migration and invasion, cell protrusion, and invasion and metastasis in model cancer xenografts. Mechanistically, PLK4 functionally targets the Arp2/3 complex, and a physical and functional interaction between PLK4 and Arp2 drives PLK4-driven cancer cell movement [17–19]. An interaction between STIL, CEP85 and PLK4 is also implicated in cytoskeletal dynamics [20], and the WNT signalling pathway represents another recently described non-canonical PLK4 target [21].

Like many Ser/Thr protein kinases, PLK activity is itself controlled by phosphorylation in the activation segment; for PLK1 this is driven through Aurora A-dependent phosphorylation at Thr210 in the PLK1 T-loop [22,23]. In contrast, PLK4 autoactivates through template-driven autophosphorylation in its activation segment, where at least six sites of autophosphorylation, notably trans-autophosphorylated Thr170 (Thr172 in flies) [4], are conserved across multiple species [6,24,25]. To evaluate potential PLK4 substrates, the active human PLK4 catalytic domain can be conveniently expressed in bacteria, where autoactivation is also mediated by autophosphorylation at multiple activation segment amino acids, including a non-canonical Tyr residue [26,27]. PLK4 possesses a triple polo box architecture that facilitates oligomerization, centriole and substrate targeting [28], and helps promote *trans*-autophosphorylation of PLK4 at multiple amino acids [29–32]. The polo box domains (PBDs) of human PLK1–3, and those from budding yeast CDC5 and Plx1 from *Xenopus laevis*, all recognise similar pS/pT-binding motifs in a proline-directed S[pS/pT]P consensus, which allows PLKs to interact with pre-phosphorylated ‘primed’ substrates as part of ordered enrichment mechanisms in cells [33].

Binding of the PLK4 substrate STIL promotes a key autophosphorylation event within the 23 amino acid phosphodegron (residues 282–305) [13]. PLK4 ubiquitination then ensues, targeting it for proteasomal-mediated degradation [6,24,25]. This process of self-destruction ensures that centriole duplication is limited to only once per cell cycle and provides an additional mechanism for temporal control of phosphorylation of downstream targets, both directly or through priming phosphorylation events [6,24,25,34]. Although additional physiological PLK4 substrates have been identified [6,14,35–38], a detailed characterisation of cellular PLK4 substrates phosphorylated during G1/S phase, or indeed across the phases of the cell cycle, is still lacking. Consequently, the contribution of PLK4 to centrosomal and non-centrosomal biology, ciliopathies and congenital abnormalities associated with gene dosage affects, alongside PLK4 kinase-independent functions that stabilise the kinase, remain to be established [6,39–41].

PLK substrate specificity has been evaluated using both proteins and peptide arrays, and a broad acidic consensus for phosphorylation by PLK1 has been established: [D/E]x[pS/pT]Φ, where x is any amino acid and Φ is an amino acid with a hydrophobic side chain [42,43]. PLK2 and PLK3 also appear to possess a preference for acidic residues adjacent to the site of phosphorylation [44], with some bias for N- and C-terminal negative charge in the canonical [D/E]x[pS/pT]xEE motif [45,46]. In contrast, PLK4 is unusual in the PLK family with respect to both substrate and small molecule specificity. Sequence and substrate similarity is highest between PLK2 and PLK3, followed by PLK1 and then PLK4, which is the least representative of the family [45]. Consistently, a dual C-terminal hydrophobic consensus ([pS/pT]ΦΦ) has been ascribed to efficient PLK4 substrate phosphorylation in the literature, based on specificity studies using (PLK1)-based optimised synthetic peptide arrays [47] and a variety of recombinant protein assays [16,38]. Consistently, many physiological PLK4 substrates conform to this broad hydrophobic consensus C-terminal to the site of modification. However, other variants of peptide substrates have also been shown to be phosphorylated by PLK4 in peptide array studies, with bias shown towards those with an Asp or Asn at the –2 position [45], as well as hydrophobic and basic amino acids C-terminal to the site of phosphorylation [45–47]. Justifiably, these findings have guided the research community in the search for distinct PLK1, 2, 3 and 4 substrates. Indeed, chemical-genetic screens and phosphospecific antibodies, have led to the identification of a variety of cellular PLK4 substrates, including STIL, CEP192 and CEP131, in vertebrate cells [16,38]. While these studies also uncovered many potential additional PLK4-dependent phosphorylation sites in presumed targets, interpretation of these data were guided by their potential localisation to the centrosome, and/or an involvement in centrosomal biology, usually with the explicit assumption that PLK4 phosphorylates sites in substrates conform to a ([pS/pT]ΦΦ) consensus.

The relatively high specificity of the cell-permeable PLK4 inhibitor centrinone [48] has led to its adoption as a tool compound for rapid PLK4 inactivation in living cells. Unlike promiscuous PLK4 inhibitors such as

CFI-400945 [49], centrinone was chemically optimised using the pan-Aurora kinase and PLK4 inhibitor VX-680 (MK-0457) [50], as the template. The addition of a methoxy substituent at the C5 position promotes interaction with Met91, lying 2 amino acids C-terminal from the gatekeeper residue Leu89 in the PLK4 hinge region [51]. This results in a reported two orders-of-magnitude increase in inhibition of PLK4 relative to Aurora A. Moreover, incubation of human cells with centrinone provides a useful approach for studying a variety of phenotypic effects [41,52], with the explicit caveat that, as with essentially all kinase inhibitors, off-target effects are inevitable. Most notably, prolonged centrinone exposure leads to the depletion of centrosomes, causing cell cycle arrest in G1 via a p53-dependent mechanism, potentially by loss of the interaction between p53 and the ubiquitin E3 ligase MDM2 [48]. Importantly, centrinone exposure of cells containing a drug-resistant PLK4 (in which Gly95, which is critical for drug-binding, is mutated to Leu) provided compelling evidence that the loss of centrosome phenotype is a direct result of PLK4 inhibition, since centrosomes are maintained normally in the presence of centrinone in the drug-resistant cell line [48]. Experimentally, the differing substrate specificity of Aurora kinases, which are primarily basophilic Ser/Thr kinases that do not tolerate Pro in the +1 position [53,54], and PLK4, which has no obvious preference for Arg/Lys N-terminal to the site of substrate phosphorylation [45,47], can also simplify the analysis of phosphoproteomics datasets generated with specific small molecules such as centrinone.

In this study, we perform an in-depth quantitative phosphoproteomics analysis to identify, in an unbiased manner, putative direct and downstream targets of PLK4. By exploiting centrinone and a previously described drug-resistant G95R PLK4 allele [55], we identify hundreds of centrinone-regulated phosphorylation sites in human U2OS cells that are sensitive to acute drug exposure. Surprisingly, phosphorylation motif analysis reveals a Pro-directed consensus in the majority of centrinone-sensitive phosphosites, which might, therefore, be dependent on PLK4 catalytic activity. Consistently, we confirm that three centrinone targets, the tyrosine phosphatase PTPN12, the neuroblastoma-driving transcription factor NMYC and PLK4 itself, are directly phosphorylated by recombinant PLK4 *in vitro*. We conclude that non-canonical Pro-directed phosphorylation sites that lie downstream of centrinone have the potential to be direct, or indirect, PLK4 targets, depending upon the substrate and context.

Materials and methods

Small molecules, reagents and antibodies

Unless otherwise stated, general laboratory reagents were purchased from Sigma–Aldrich and were of the highest quality available. The following antibodies were used: anti-PLK4 antibody clone 6H5 (Millipore, used at 1/100 for western blot and immunofluorescence), anti-Aurora A (Cell Signaling Technologies, 1/5000 for western blot, 1/500 for immunofluorescence), anti-pericentrin (Abcam, 1/500 for immunofluorescence), anti- γ -tubulin (1/500 for immunofluorescence), anti-9E10 anti-myc (Invitrogen, 1/100 for immunofluorescence), anti-FLAG (Sigma, 1/1000 for western blot), anti- α -tubulin (TAT1) (1/5000 for western blot), anti-GAPDH (1/5000 for western blot). N-terminally FITC-coupled (fluorescent) PLK4, NMYC, PTPN12 and CEP131 substrate peptides were designed for EZ reader assays in-house and purchased from Pepceuticals, Leicester, U.K. (see Table 1 for parental peptides). Centrinone and VX-680 were obtained as previously described [56].

Cell culture and generation of stable cell lines

U2OS T-REx parental FLP-In cells were maintained in DMEM supplemented with 10% (v/v) foetal bovine serum, penicillin (100 U/ml), streptomycin (100 U/ml) and L-glutamine (2 mM), 0.1 mg/ml Zeocin and 15 μ g/ml blasticidin at 37°C, 5% CO₂. Stable cells were generated based on published protocols using the FLP recombinase plasmid pOG44 [2,7]. Briefly, tetracycline-inducible lines expressing either MYC or FLAG-tagged PLK4 were initially generated by transfection of parental T-REx cells (a kind gift of Dr Gopal Sapkota, University of Dundee). Stable U2OS clonal populations that contained either FLAG-WT PLK4, FLAG G95R PLK4, MYC-WT PLK4 or MYC-G95R PLK4 were established by selection for 2–3 weeks with 15 μ g/ml blasticidin and 100 μ g/ml hygromycin B, as described for other U2OS models [55,57–59], and FLAG-PLK4 or MYC-PLK4 expression was induced by the addition of 1 μ g/ml tetracycline. Cells were maintained in culture and split at ~80% confluence, when cells were washed with PBS, trypsinised (0.05% (v/v)) and harvested by centrifugation at 220 \times g.

Table 1. PLK4 enzyme assays and substrates

Substrate sequence	Parental substrate sequence
Human PLK4 (bacteria)	Amino acids 1–269
Human PTPN12 (wheat germ cell free)	Amino acids 1–780
Human NMYC (wheat germ cell free)	Amino acids 1–464
PLK4 CDK7/CAK substrate	5FAM-FLAKSFGSPNRAYKK-CONH ₂
PLK4 polybasic ('RK') substrate	5FAM-RKKKSFYFKKHHH-CONH ₂
NMYC substrate	5FAM-KFELLPTPLSPSR-CONH ₂
PTPN12 substrate	5FAM-TVSLTPSPPTQVET-CONH ₂
CEP131 substrate 1	5FAM-NLRRSNSTTQVSQ-CONH ₂
CEP131 substrate 2	5FAM-SQPRSGSPRPTEP-CONH ₂

Sequence of recombinant protein kinases and peptide substrates employed for assay of recombinant human PLK4. Sources of enzymes are included. 5FAM = 5-carboxyfluorescein.

Immunofluorescence microscopy

U2OS FLAG-WT PLK4, FLAG G95R PLK4, MYC-WT PLK4 or MYC-G95R PLK4 stably transfected cells were split into a six well plate containing cover slips. At ~80% confluence, 1 µg/ml tetracycline was added to induce protein expression for 18 h. Cells were washed with 2.5 ml PBS and fixed for 20 min with 2.5 ml of 3.7% (v/v) paraformaldehyde. Cells were then washed 3× with 2.5 ml PBS and permeabilised with 0.1% (v/v) Triton X-100 for 10 min. Cells were washed a further 3× with PBS and blocked with 1% (w/v) BSA in 0.3 M glycine for 60 min, and washed twice with PBS. Primary antibodies, 9E10 anti-myc antibody (1/100), anti-γ-tubulin (1/5000) or anti-pericentrin (1/500) in 500 µl of 1% (w/v) BSA were added to each coverslip and incubated overnight at 4°C in a humidified chamber. Cells were washed 5× for 10 min with PBS, prior to incubation for 1 h (RT, dark) with secondary antibody (rabbit anti-mouse-Cy3 or goat anti-rabbit-FITC, 1 in 200 dilution). Cells were washed 5 × 5 min with PBS and incubated with 1 µg/ml DAPI for 3 min. Coverslips were mounted onto microscope slides and secured with immune-mount and imaged on a Zeiss LSM 880 confocal microscope using an alpha Plan-Apochromat 100×/1.46 DIC grade oil immersion lens. A 405 nm diode, 488 nm Argon and 561 nm diode laser were used to excite DAPI, Alexa 488 and Cy3 respectively with a transmitted light image also captured. A pinhole of ~1 Airy unit was maintained throughout imaging. Spatial sampling was conducted using Nyquist sampling for the chosen magnification with four times line averaging used to reduce noise. For each condition at least one z-stack through the sample was acquired with slices taken at ~1 µm throughout the cell under investigation.

Flow cytometry (FACS)

U2OS FLAG-WT and G95R PLK4 cells were split into 10 cm² dishes. At 60% confluence, cells were incubated with 1 µg/ml tetracycline (18 h) before the addition of centrinone (300 nM) or vehicle control for 4 h. Cells were washed with PBS and released with trypsin (0.05% (v/v)). Following centrifugation at 220×g, PBS was removed and cells fixed with 70% (v/v) ethanol, added slowly whilst vortexing to avoid aggregation, and stored at –20°C overnight. Fixed cells were washed with PBS and incubated with 200 µl Guava cell cycle reagent for 30 min (RT, dark). Samples were transferred to a 96-well plate and analysed using a Guava easycyte HT cytometer. ANOVA statistical analysis and Tukey *post-hoc* testing were performed in R.

SILAC labelling

U2OS T-REx Flp-in cells stably transfected with FLAG-WT PLK4 or FLAG-G95R PLK4 were grown in DMEM supplemented with 10% (v/v) dialysed foetal bovine serum, penicillin (100 U/ml) and streptomycin (100 U/ml). Once 80% confluency was reached, cells were split in to DMEM containing 'heavy' labelled, ¹⁵N₂¹³C₆-lysine (Lys8) and ¹⁵N₄¹³C₆-arginine (Arg10) for approximately seven cell doublings to permit full incorporation of the label. At 80% confluence, cells were washed with PBS, released with trypsin (0.05% (v/v)) and centrifuged at 220×g.

Cell lysis

For immunoblotting, cells were lysed in 1% (v/v) NP-40, 1% (w/v) SDS dissolved in 50 mM Tris-HCl pH 8.0 and 150 mM NaCl, supplemented with Roche protease inhibitor cocktail tablet. The lysate was sonicated briefly and centrifuged at 15 000×g (4°C) for 20 min. Protein concentration was quantified using the Bradford Assay (Bio-Rad). For co-immunoprecipitation (IP) experiments, cells were lysed in 50 mM Tris-HCl (pH 8.0), 150 mM NaCl, 0.5% NP-40, 1 mM DTT, 2 mM MgCl₂, and benzonase supplemented with a protease inhibitor (Roche) cocktail tablet. After 30 min incubation on ice, cell lysates were clarified by centrifugation (15 000×g, 4°C, 20 min). For LC-MS/MS analysis, cells were lysed with an MS compatible buffer (0.25% (v/v) RapiGest SF (Waters) in 50 mM ammonium bicarbonate, supplemented with PhosStop inhibitor (Roche). Lysates were sonicated briefly to shear DNA and centrifuged (15 000×g, 4°C, 20 min).

FLAG-PLK4 immunoprecipitation

Anti-FLAG M2 Affinity Agarose resin (Sigma, ~30 µl) was washed 3× with 50 mM Tris-HCl (pH 8.0) and 150 mM NaCl and then incubated with clarified cell lysate overnight at 4°C with gentle agitation. Agarose beads were collected by centrifugation at 1000×g for 1 min and then washed 5× with 50 mM Tris-HCl (pH 8.0) containing 150 mM NaCl. Precipitated (bead-bound) proteins were eluted by incubation with 2× SDS sample loading buffer for 5 min at 98°C.

Sample preparation for (phospho)proteome analysis

SILAC-labelled protein lysates (1 mg total protein) were mixed with an equal amount of unlabelled protein lysate prior to sample preparation for LC-MS/MS analysis. Proteins were reduced, alkylated, digested with trypsin and desalted using standard procedures [60]. For high-pH reversed-phase (RP) HPLC, tryptic peptides were resuspended in 94.5% (v/v) buffer A (20 mM NH₄OH, pH 10), 5.5% (v/v) buffer B (20 mM NH₄OH in 90% acetonitrile) and loaded on to an Extend C18 (3.5 µm, 3 mm × 150 mm) Agilent column. Peptides were eluted with an increasing concentration of buffer B: to 30% over 25 min, then 75% B over 12 min, at a flow rate of 0.5 ml/min. Sixty 500 µl fractions were collected, partially dried by vacuum centrifugation and concatenated to 12 pools. Aliquots (5 µl) were removed from each of the 12 × 50 µl pools for total proteomic analysis, and the remaining sample (45 µl) was subjected to TiO₂-based phosphopeptide enrichment as previously described [60].

LC-MS/MS

Reversed-phase capillary HPLC separations were performed using an UltiMate 3000 nano system (Dionex) coupled in-line with a Thermo Orbitrap Fusion Tribrid mass spectrometer (Thermo Scientific, Bremen, Germany) as described [60]. For proteome analysis, full scan MS1 spectra were acquired in the Orbitrap (120k resolution at *m/z* 200) using a top-speed approach (3 s cycle time) to perform for HCD-mediated fragmentation with a normalised collision energy of 32%. MS2 spectra were acquired in the ion trap. Phosphopeptide analysis was performed [60] using the HCD orbitrap method, where both MS1 and MS2 spectra were acquired in the orbitrap (60k resolution for MS1, 30k resolution for MS2).

(Phospho)proteomics data processing

Phosphopeptide data were processed using Andromeda with PTM-score implemented within MaxQuant (version 1.6.0.16) [61]. MS/MS spectra were searched against a database containing the human UniProt database (downloaded December 2015; 20 187 sequences). Trypsin was set as the digestion enzyme and two missed cleavages were permitted. Cysteine carbamidomethylation was set as a fixed modification. Variable modifications were set as oxidation (M), phospho (S/T/Y). Default instrument parameters and score thresholds were used: MS1 first search peptide tolerance of 20 ppm and main search tolerance of 4.5 ppm; FTMS MS2 tolerance of 20 ppm; ITMS MS2 tolerance of 0.5 Da. A false discovery rate (FDR) of 1% for peptide spectrum matches (PSM) and proteins was applied. For processing of SILAC data, Thermo files (.raw format) were loaded in to MaxQuant (version 1.6.0.16). Total proteomics (protein expression data) and phosphoproteomics experiments were processed separately. The experimental template design separated individual bioreplicates into separate experiments, linking the experiment to the relevant fractions. MaxQuant parameters were as described above, with the following additions: 'multiplicity' was set to 2 and Arg10/Lys8 were selected as labels. For proteomics datasets, the variable modifications oxidation (M), acetyl (protein N-term) were included. Both 'requantify' and

‘match between runs’ were enabled. At least two peptides were required for protein quantification. Post processing was performed using Perseus (version 1.6.0.7). For proteingroups.txt output files, Perseus was used to filter out contaminants, reverse decoy hits and those ‘matched only by site’. Additionally, data were filtered to include proteins identified in ≥ 3 (out of 4) bioreplicates and Log_2 transformed. For phosphosites(STY).txt output files, data were filtered as above. In addition, ‘expand site table’ feature was used to separate individual phosphosites, and a phosphosite localisation cut-off of ≥ 0.75 was applied. Ratios were Log_2 transformed. Statistical analysis was then performed using the LIMMA package in R with Benjamini–Hochberg multiple corrections to generate adjusted *p*-values.

Evolutionary conservation

To calculate evolutionary conservation of the most confidently localised phosphosite per phosphopeptide, the sequences of leading assigned proteins for all phosphopeptides were used as a query in a protein–protein BLAST [62] search (BLAST 2.9.0+ version; 11/03/19 build) against the proteomes of 100 eukaryotic species (50 mammals, 12 birds, 5 fish, 4 reptiles, 2 amphibians, 11 insects, 4 fungi, 7 plants and 5 protists) downloaded from UniProt (November 2019) — see Supplementary Table S2 for full proteome descriptions. For each target protein, a top orthologue was extracted from each species (*E*-value ≤ 0.00001). The orthologues were aligned with the target protein using MUSCLE [63] (version 3.8.31). From the alignments, percentage conservation was calculated for each Ser, Thr and Tyr residue within the sequence of each target protein out of 100 (all proteomes), and out of the number of aligned orthologues. Additional conservation percentages were calculated taking into account Ser/Thr substitutions in orthologues, whereby an orthologue is included in % conservation calculation if, for example, a Thr from an orthologue is aligned with a target Ser and vice versa. Furthermore, conservation percentages were given for -1 and $+1$ sites around each Ser, Thr and Tyr in target sequence across aligned orthologues. All conservation data was then cross-referenced with phosphopeptide data to determine the conservation of target sites. The most confident phosphosite per phosphopeptide was also cross-referenced against data from PeptideAtlas (PA) [64] (2020 build), and from PhosphoSitePlus (PSP) [65] (11/03/20 build), both of which had been pre-processed to categorise previously observed phosphorylation site confidence categories, based on the number of observations (‘High’: ≥ 5 previous observations, very likely true site; ‘Medium’: 2–4 previous observations, likely true site; ‘Low’: 1 previous observation, little support that it is a true site; PA only — ‘Not phosphorylated’: frequently (>5) observed to be not phosphorylated, never observed as phosphorylated; ‘Other’ — no confident evidence in any category). Observations in PA were counted with a threshold of >0.95 PTM Prophet probability for positive evidence, and ≤ 0.19 for evidence of not being phosphorylated.

Icelogo analysis

Cellular phosphosites that were modulated after centrinone treatment were aligned to the centre of a sequence window composed of five amino acids *N*- and *C*-terminal to the mapped phosphorylation site. Sequence motif logos were generated with IceLogo v1.2 [66] using percentage difference against a background of the precompiled human SwissProt composition and a *p*-value cut-off of 0.05.

Functional enrichment analysis

Proteins and phosphoproteins that were significantly altered in response to centrinone were subjected to functional enrichment analysis using the DAVID Bioinformatics Resources (v6.8) [67,68]. ‘clusterProfiler’ R package was used to create dotplots from these datasets, where *p*-values, enrichment factor, protein count and functional category could be presented.

Network analysis

Significantly down-regulated proteins from the G95R PLK4 SILAC dataset (adj. *p*-value < 0.05) were submitted to the STRING database (v. 10.5) to assess protein–protein interactions [69]. A high confidence (score 0.7) filter was applied, and only ‘experiments’ and ‘databases’ as active interaction sources were included.

Expression and purification of PLK4 catalytic domain

6His-*N*-terminally tagged human PLK4 catalytic domain (amino acids 1–269) was expressed and purified in bacteria as described previously and affinity purified using Ni-NTA agarose [27]. Proteins were eluted from beads by incubation with buffer containing 0.5 M imidazole. PLK4 amino acid substitutions were introduced

using standard PCR-based site-directed mutagenesis protocols and confirmed by sequencing the whole PLK4 1–269 coding region.

DSF (differential scanning fluorimetry) assays

Thermal shift assays were performed on a StepOnePlus Real-Time PCR machine (Life Technologies) in combination with Sypro-Orange dye (Invitrogen) and a thermal ramping protocol (0.3°C per minute between 25 and 94°C). Recombinant PLK4 proteins were assayed at 5 µM in 50 mM Tris–HCl (pH 7.4) and 100 mM NaCl in the presence or absence of the indicated concentrations of ligand or inhibitor compound [final DMSO concentration 4% (v/v)]. Data were processed using the Boltzmann equation to generate sigmoidal denaturation curves, and average $T_m/\Delta T_m$ values were calculated as described using GraphPad Prism software [70].

PLK4 phosphorylation assays

All *in vitro* peptide-based enzyme assays were carried out using the Caliper LabChip EZ Reader platform, which monitors phosphorylation-induced changes in the mobility of a fluorescently labelled PLK4 peptide substrate [27,71,72]. To assess PLK4 activity, WT or G95R PLK4 (0.5–10 µg, depending upon the assay) were incubated with 1 mM ATP (to mimic cellular concentration) and 2 µM of the appropriate fluorescent peptide substrate in 25 mM HEPES (pH 7.4), 5 mM MgCl₂, and 0.001% (v/v) Brij 35. Centrinone-mediated enzyme inhibition was quantified under identical assay conditions using WT or G95R PLK4 (5 µg), in the presence of increasing concentrations of centrinone (10 nM to 100 µM) by monitoring the generation of phosphopeptide during the assay, by real-time peak integration and quantification of relative amounts of peptide and phosphopeptide. Data were normalised with respect to control assays, with pmoles of phosphate incorporated into the peptide generally limited to <20% of maximum, in order to prevent depletion of ATP, end product effects and to ensure assay linearity. Reactions were pre-incubated for 30 min at 37°C prior to the addition of ATP. The following peptide substrates (Table 1) were synthesised, lyophilised, and reconstituted in DMSO prior to use at a fixed concentration in PLK4 kinase assays. The human sequence-derived regions for the peptide substrates are: CDK7/CAK (amino acids 158–169) FLAKSFGSPNRAYKK and point mutants FLAKAFGSPNRAYKK, FLAKSFGSPNAAYKK, and FLAKAFGAPNRAYKK, polybasic ‘RK’ substrate RKKKSFYFKKHHH and F6P substitution RKKKSPYFKKHHH, CEP131 (amino acids 72–84) substrate peptide 1, NLRRSNSTTQVSQ (and point mutant NLRRSNATTQVSQ), and CEP131 (amino acids 83–95) substrate peptide 2, SQPRSGSPRPTEP (and point mutant SQPRSGAPRPTEP), NMYC (amino acids 52–65) substrate KFELLTPPLSPSR (and point mutants KFELLPAPPLSPSR, KFELLPTPLAPSR, KFELLPAPPLAPSR and KFELLPTAPLSASR) and PTPN12 (amino acids 565–578) substrate TVSLTPSPTTQVET (and point mutants TVSLAPSPTTQVET, TVSLTPAPTTQVET, TVSLAPAPTTQVET and TVSLTASATTQVET). Where indicated, phosphorylation of peptides by the active Pro-directed kinase GST-CDK2/Cyclin A2 (100 ng purified from Sf9 cells, Sigma) was also confirmed in the presence or absence of the ATP competitive inhibitor, Purvalanol A (100 µM). The phosphorylation kinetics of GST-NMYC (full length, amino acids 1–464) or GST-PTPN12 (amino acids 1–780), both expressed in wheatgerm cell-free systems (Abcam), were measuring through PLK4-dependent phosphate incorporation from gamma-³²P-labelled ATP. WT PLK4 (2 µg) was incubated with 2 µg of either substrate protein and assayed in 50 mM Tris, pH 7.4, 100 mM NaCl, and 1 mM DTT in the presence of 200 µM ATP (containing 2 µCi ³²P ATP per assay) and 10 mM MgCl₂ at 30°C. The reactions were terminated at the indicated time points by denaturation in SDS sample buffer prior to separation by SDS–PAGE and transfer to nitrocellulose membranes. ³²P-incorporation into PLK4 (autophosphorylation) was detected by autoradiography. Equal loading of appropriate proteins was confirmed by Ponceau S staining and destaining of the membrane. To evaluate site-specific phosphorylation, trypsin proteolysis, TiO₂-based phosphopeptide enrichment and liquid chromatography-tandem mass spectrometry (LC–MS/MS) analysis was performed using an Orbitrap Fusion mass spectrometer (Thermo Scientific, Bremen) as previously described [60], with enrichment being performed using Titansphere Phos-TiO tips (GL Sciences), as per the manufacturer’s instructions.

Results

Inducible stable U2OS cell lines to investigate dynamic PLK4 signalling using the small molecule inhibitor centrinone

To quantify PLK4 signalling pathways in intact cells, we set out to perform a quantitative investigation of the dynamic phosphoproteome of human cells following treatment with the inhibitor centrinone. Importantly, this

chemical has been reported to be a specific inhibitor of PLK4, exhibiting high specificity for this Ser/Thr protein kinase compared with the related kinase Aurora A (Figure 1A). To evaluate potential off-target effects of centrinone inhibition we initially exploited a chemical-genetic approach, generating stable isogenic tetracycline-inducible U2OS cell lines expressing either wild-type (WT), or drug-resistant (G95R), N-terminally epitope-tagged PLK4, in the presence of the endogenous PLK4 gene. This strategy allowed us to inducibly control PLK4 protein levels for robust detection and quantification of putative PLK4 substrates, including PLK4 itself, which is expressed at very low (sometimes undetectable) levels in the parental cell line. Mutation of the Gly95 residue of PLK4 to Arg results in a catalytically active enzyme that is resistant to concentrations of up to 100 μ M centrinone *in vitro*, in the presence of cell-mimicking concentrations (1 mM) of the ATP cofactor (Supplementary Figure S1A–D). Under these experimental conditions, which are designed to mimic the cellular environment, centrinone possessed an IC_{50} of ~ 330 nM for WT PLK4 (Supplementary Figure S1D). Consistently, the generation of PLK4 (1–269) containing the G95R substitution expressed in bacteria did not significantly change *in vitro* autophosphorylation at multiple regulatory sites, including the activating residue T170, or its specific activity towards a synthetic fluorescent PLK4 peptide substrate (Supplementary Figure S1C). However, as expected, we observed a marked reduction in inhibition of the G95R PLK4 protein

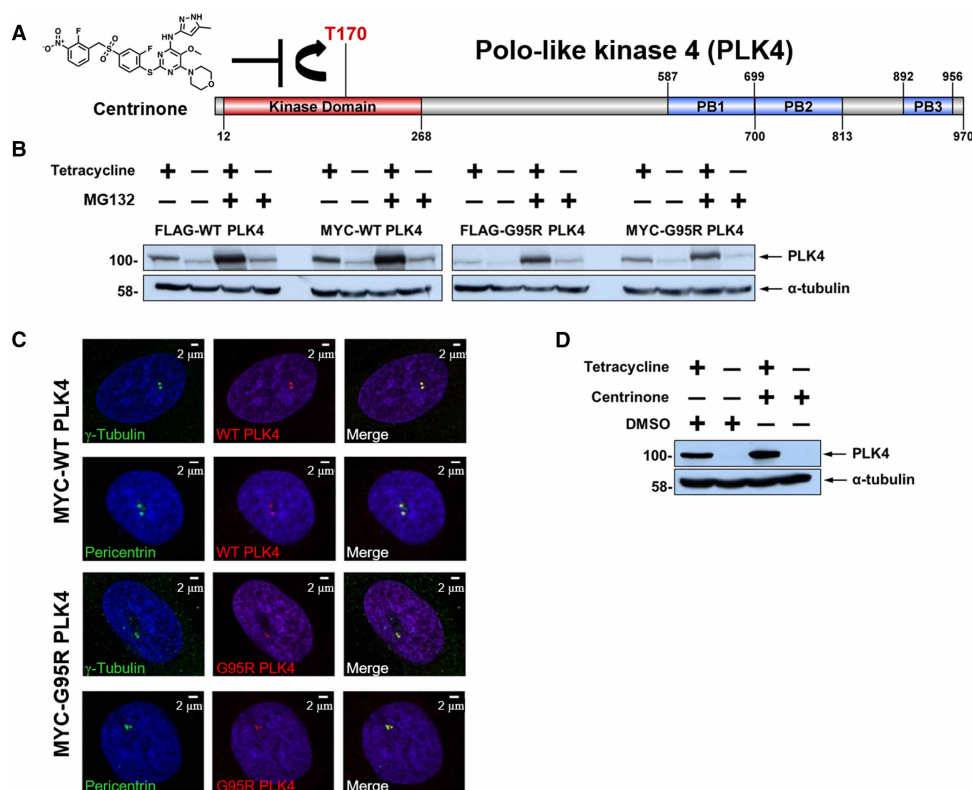


Figure 1. Generation and characterisation of stable inducible cell lines expressing WT or G95R PLK4.

(A) Structure of the PLK4 inhibitor centrinone and schematic of human PLK4 domain structure. Residues that demarcate the kinase domain, T170 site of activating phosphorylation, and the three polo box domains are indicated. (B) U2OS cells stably transfected with either FLAG- or MYC-tagged WT or G95R PLK4 were incubated in the presence or absence of tetracycline (1 μ g/ml) for 18 h to induce PLK4 expression, followed by MG132 (10 μ M) for 4 h. Lysates were probed with antibodies that recognise either PLK4 or α -tubulin as a loading control. (C) U2OS cells induced to express MYC-PLK4 (WT or G95R) with tetracycline were probed with anti-PLK4 (red) and either anti- γ -tubulin or anti-pericentrin (green) antibodies and analysed by immunofluorescence microscopy, confirming localisation of both WT and G95R PLK4 at the centrosome. (D) U2OS cells stably transfected with FLAG-WT PLK4 were incubated in the presence or absence of tetracycline (1 μ g/ml) for 18 h. Cells were then treated with 300 nM centrinone or DMSO (0.1% v/v) for 4 h. Lysates were analysed by western blot and probed with antibodies against either PLK4 or α -tubulin as a loading control.

(Supplementary Figure S1D) by centrione, and centrione (and VX-680)-dependent stabilisation of G95R PLK4 protein was decreased by over 75% compared with PLK4 protein, as judged by DSF analysis. These data are consistent with a very significant decrease in PLK4 G95R binding to centrione, but not Mg-ATP (Supplementary Figure S1E), which is predicted to manifest as cellular centrione drug-resistance in the presence of physiological levels of competing ATP.

We next validated inducible expression in WT and G95R PLK4 stable cell lines following incubation with tetracycline, in the absence and presence of the proteasome inhibitor, MG132, which prevents proteasome-mediated degradation of ‘suicide’ kinases such as PLK4 (Figure 1B; Supplementary Figure S2). As determined by immunoblotting, both WT and G95R PLK4 expression was induced by tetracycline in all cell lines, with protein levels increasing, as expected, in the presence of MG132. Comparable levels of recombinant PLK4 expression were detected when fused to either an N-terminal MYC or FLAG tag (Figure 1B). By immunofluorescence in fixed cells, we also confirmed that the overexpressed MYC-PLK4 (both WT and G95R) correctly localised to centriolar structures (co-localising with pericentrin and γ -tubulin) during interphase (Figure 1C). Having generated a new cellular system for controlled overexpression of either WT PLK4 or G95R PLK4, the cellular effects of centrione inhibition were assessed after Tet-exposure in FLAG-PLK4 lines, which are the focus of the proteomic studies reported below. PLK4 controls its own proteasome-mediated degradation through autophosphorylation of Ser293 and Thr297 in the degron domain [6]; inhibition of PLK4 activity with centrione should, therefore, result in PLK4 protein accumulation. As expected, centrione treatment of stably transfected FLAG-PLK4 increased tetracycline-dependent PLK4 expression levels (Figure 1D). Owing to the high promiscuity of most ATP-dependent protein kinase inhibitors [73,74], we next established optimal conditions (inhibitor concentration and length of compound-exposure) for inhibition of PLK4 activity, based on the assessment of PLK4 stability, in an attempt to minimise off-target effects. To this end, we exposed WT PLK4 U2OS cells to centrione and examined FLAG-PLK4 expression at various time points over a 24 h period (Supplementary Figure S2A). As expected, treatment of the WT PLK4 line with centrione resulted in time-dependent accumulation of FLAG-PLK4 protein, which was maximal at 300 nM centrione, similar to MG132 treatment. This observation is consistent with the inhibition of PLK4 autophosphorylation sites that promote SCF-dependent proteasomal degradation [6]. In contrast, centrione treatment of FLAG-G95R PLK4 U2OS cells did not result in a marked increase in exogenous PLK4 protein, even at the highest concentration (1 μ M) of centrione tested (Supplementary Figure S2B, right panel). These cell models, therefore, provide a centrione-regulated PLK4-expressing system, which can be used to potentially identify and evaluate PLK4-dependent phosphorylation events and associated signalling pathways.

SILAC-based centrione (phospho)proteomics screen

To evaluate centrione-dependent signalling, and help discover potential new PLK4 substrates, we undertook a global quantitative phosphoproteomics screen using the inducible FLAG-WT PLK4 and FLAG-G95R PLK4 U2OS cell lines. Similar global (phospho)proteomics analyses in the presence of kinase inhibitors have been performed previously to evaluate the cellular activities of PLK1 and Aurora A, revealing phosphorylation sites linked to activity during mitotic progression in HeLa cells [75,76]. Using a SILAC-based quantification strategy, we evaluated protein and phosphopeptide level regulation following tetracycline induction of FLAG-PLK4 in the absence or presence of centrione, but in the absence of experimental cell cycle arrest (Figure 2A). The efficiency of protein metabolic labelling using ‘heavy’ (R10K8) SILAC media was determined after each cell doubling, and was found to exceed 96%. We also confirmed a lack of significant metabolic conversion [77] of isotopically labelled Arg to Pro (Supplementary Figure S3). Cells expressing either WT PLK4 or G95R PLK4 were exposed to compounds and harvested after approximately seven cell doublings, and lysates for a given cell line were combined for tryptic proteolysis. To improve the depth of coverage of the (phospho)proteome, tryptic peptides were subjected to high-pH reversed-phase chromatography, collecting 60 fractions which were concatenated into 12 pools. A proportion (90%) of these pooled fractions subsequently underwent TiO_2 -based phosphopeptide enrichment and LC-MS/MS analysis, retaining the remaining portion of each sample for comparative total protein quantification (Figure 2A). A high degree of overlap was observed across the four biological replicates, with 96% of the 7354 expressed gene products identified in the FLAG-WT PLK4 cell line (at a FDR of <1%) being observed in three or more replicates, meaning that a total of 6046 (82%) proteins could be quantified (Figure 2B). Not unexpectedly, due to the stochastic nature of data-dependent acquisition (DDA), reproducibility at the phosphopeptide level was lower, with ~71% of the 13 816 phosphopeptides identified in

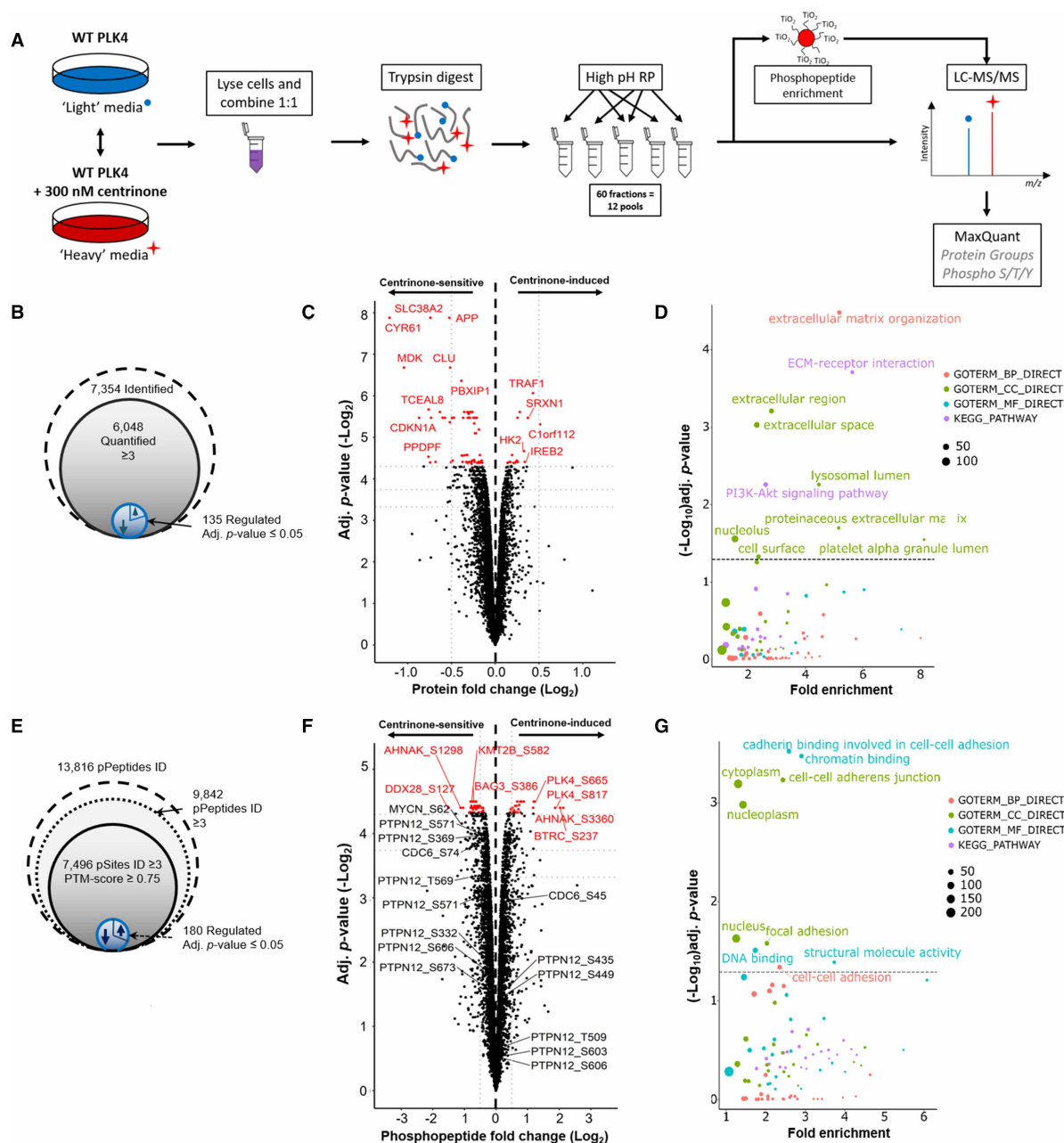


Figure 2. Identification of centrinone-regulated changes in the proteome and phosphoproteome of human cells. Part 1 of 2
(A) Workflow for SILAC-based quantitative analysis of centrinone-mediated regulation of the proteome and the phosphoproteome of FLAG-WT PLK4 U2OS cells. Following induction of FLAG-WT PLK4 with tetracycline (1 $\mu\text{g}/\text{ml}$) for 18 h, cells were treated with either 300 nM centrinone ('heavy' labelled) or DMSO (0.1% v/v) control (unlabelled) for 4 h, prior to protein extraction and tryptic proteolysis. Peptides were separated by high-pH reversed-phase chromatography into 12 pools, concatenated from 60 fractions. 90% of each pool was subjected to TiO_2 -based phosphopeptide enrichment. Enriched and non-enriched samples were then subjected to LC-MS/MS using an Orbitrap Fusion mass spectrometer. Data were analysed using MaxQuant software. Total numbers of identified, quantified and differentially regulated (B) proteins or (E) phosphosites are indicated. Volcano plots showing (C) protein or (F) phosphopeptide fold ratios following Bayesian statistical analysis to evaluate significant differences. Log_2 -fold change (Heavy/Light) are presented as a function of the $-\text{Log}_2$ Benjamini-Hochberg adjusted p -value; those with an adjusted p -value ≤ 0.05 are highlighted in red. Select data points of note are annotated with their protein accession number (and differentially regulated phosphosite in the case of phosphopeptide analysis). (D,G) GO term enrichment analysis of significantly regulated proteins (D) or phosphosites (G) using DAVID. Proteins/phosphopeptides with a Benjamini-Hochberg adjusted p -value ≤ 0.05 are labelled.

Figure 2. Identification of centrinone-regulated changes in the proteome and phosphoproteome of human cells. Part 2 of 2
 BP = biological process (red); CC = cellular compartment (green); MF = molecular function (cyan); KEGG pathway (purple). The size of the node is representative of the number of proteins contributing to a select category.

the WT-PLK4 cells being observed in at least three of the biological replicates. Of these, 7496 sites of phosphorylation, localised at a PTM-score ≥ 0.75 , were quantified across at least three bioreplicates (Figure 2E).

At the proteome level, 135 proteins were significantly up or down-regulated upon centrinone treatment of FLAG-WT PLK4 cells, using an adjusted p -value ≤ 0.05 , with the level of 100 proteins decreasing, compared with 35 increasing, in the presence of centrinone (Figure 2B,C and Supplementary Table S1). Importantly, PLK4 itself was up-regulated 1.8-fold (p -value = 1.0×10^{-03} , adj. p -value = 0.05) in the presence of centrinone, consistent with the accumulation of PLK4 under these conditions, as evidenced by immunoblotting (Figure 1D). PLK4 was the only protein that was significantly up-regulated (p -value ≤ 0.05) with a greater than 1.5-fold change, although 15 proteins were down-regulated (>1.5 -fold) under the same conditions, including cyclin-dependent kinase inhibitor 1 (1.8-fold; p -value = 1.3×10^{-04} , adj. p -value = 2.3×10^{-02}) and its binding partner cyclin D2 (1.7-fold; p -value = 5.8×10^{-04} , adj. p -value = 4.8×10^{-02}). Consistent down-regulation of the cyclin D2 regulator, CDK4 (1.14-fold, p -value = 1.1×10^{-03} , adj. p -value = 5.3×10^{-02}) was also observed, and the related protein CDK6 was also up-regulated under the same conditions (1.16-fold, p -value = 6.4×10^{-04} , adj. p -value = 4.8×10^{-02}). These findings are representative of the several new centrinone targets that are associated with G1/S phases of the cell cycle, downstream of PLK4 inhibition. Functional annotation and enrichment analysis of the centrinone-mediated changes in protein abundance using DAVID [67,68] (Figure 2D; Supplementary Figure S4) revealed differential regulation of proteins in many distinct cellular compartments including the extracellular region, lysosomal lumen and nucleolus. Proteins involved in extracellular matrix organisation and ECM-receptor interactions were notably down-regulated following centrinone treatment, while nucleolar proteins and those involved in RNA processing/binding were significantly up-regulated (Supplementary Figure S4).

Surprisingly, many more proteins were dysregulated after centrinone treatment in the G95R PLK4 cell line when compared with the WT PLK4-expressing cells (Supplementary Figure S5). Of the 5949 proteins quantified in the FLAG-G95R PLK4-expressing cells after centrinone exposure, 1882 were significantly changed (at an adj. p -value ≤ 0.05). Of these, 585 were up-regulated, while 1297 proteins were down-regulated at the expression level. Functional annotation and enrichment analysis of the centrinone-mediated changes in protein abundance using DAVID revealed differential regulation of proteins localised in the mitochondrion, at focal adhesions and within the cell–cell adherens junctions (Supplementary Figure S5). The GO term ‘metabolic pathway proteins’, specifically those involved in amino acid biosynthesis and ribosome biogenesis, was also enriched, suggesting initiation of a cellular stress response. Proteins involved in cytokinesis and metaphase plate progression were also dysregulated.

Interestingly, several known mitotic proteins were significantly down-regulated in G95R PLK4-expressing cells, including Aurora A (1.6-fold, p -value = 6.0×10^{-05} , adj. p -value = 4.9×10^{-03}), TPX2 (1.6-fold, p -value = 7.7×10^{-06} , adj. p -value = 3.5×10^{-03}), cyclin B1 (1.6-fold, p -value = 9.2×10^{-07} , adj. p -value = 2.7×10^{-03}), cyclin B2 (1.4-fold, p -value = 4.2×10^{-03} , adj. p -value = 2.4×10^{-03}) and FOXM1 (1.5-fold, p -value = 6.1×10^{-06} , adj. p -value = 3.0×10^{-03}), suggesting centrinone effects on a G2/M regulatory protein network. Depletion of sororin (1.6-fold, p -value = 3.1×10^{-06} , adj. p -value = 3.0×10^{-03}) and CDC20 (1.6-fold, p -value = 8.9×10^{-06} , adj. p -value = 3.8×10^{-03}), key regulators of sister chromatid cohesion, and borealin (CDCA8; 1.5-fold, p -value = 1.1×10^{-05} , adj. p -value = 3.8×10^{-03}), a component of the mitotic CPC complex, also implicates a negative effect of centrinone on chromosome cohesion in clonal G95R PLK4 cells. Functional network analysis using STRING [69] revealed a broader connection between these down-regulated G2/M-phase proteins (Supplementary Figure S5D) suggesting that centrinone exposure targeted pathways controlling a broad spectrum of cell cycle regulators. Interestingly, many of those were not identified in WT PLK4-expressing cells, consistent with the presence of newly engaged non-PLK4 ‘off-targets’ (including several linked to Aurora A and G2/M phase) in cells expressing the centrinone-resistant PLK4 mutant.

Flow cytometry-based analysis of the cell cycle distribution of U2OS cells following induction of either WT PLK4 or G95R PLK did not reveal significant changes in G1 or G2/M cell cycle distribution (ruling-out induced kinase activities that are found in these phases), although both tetracycline (which leads to increased WT and G95R PLK4 expression) and centrinone (chemical PLK4 inhibition) induced subtle S-phase enrichment (Figure 3). Overall, these data are consistent with the protein level changes observed in both cell lines,

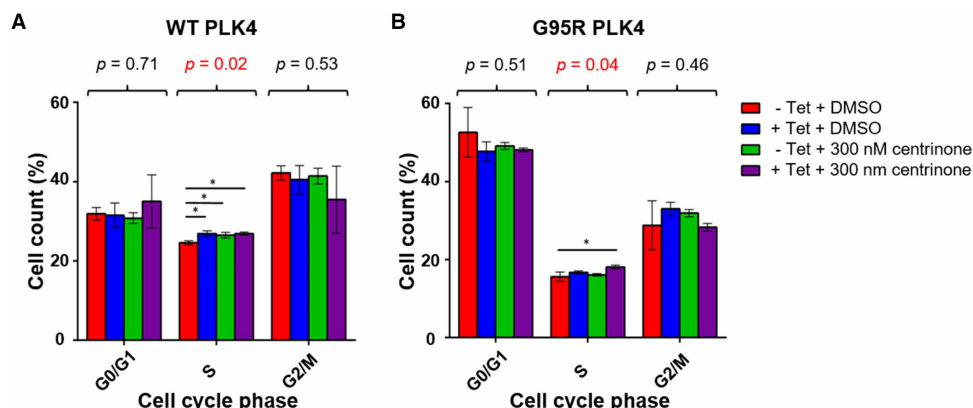


Figure 3. Centrinone induces a subtle S-phase delay in both WT and G95R PLK4 U2OS cells.

Expression of FLAG-PLK4 was induced upon incubation with 1 μ g/ml tetracycline for 18 h. Cells were treated with 300 nM centrinone or 0.1% (v/v) DMSO for 4 h and cell cycle distribution analysed by FACS. The bar chart reflects the percentage of cells (mean \pm SD, $n = 3$) in each cell cycle phase for WT (A) and G95R (B) PLK4. ANOVA generated p values are shown above each phase. * indicates significant differences between individual samples determined using Tukey *post-hoc* testing (adj. p -value ≤ 0.05).

with a small increase in S-phase cells suggesting either a slight S-phase delay, or the early onset of mitotic arrest. Further work is needed to tease apart the ‘on’ (PLK4) and ‘off’ (non-PLK4) targets of centrinone in cells that become engaged under these conditions. However, the comparatively few proteins whose levels are regulated upon centrinone treatment in the WT PLK4 cell line ($\sim 1\%$ of total) compared with the G95R PLK4 cell line ($\sim 30\%$ of total), combined with our chemical-genetic confirmation of centrinone as an on-target PLK4 inhibitor, leads to an interesting observation; in G95R PLK4 cells in the absence of its ‘preferential’ exogenous binding partner WT-PLK4, centrinone also induces destabilisation and dephosphorylation of multiple off-targets. We hypothesise (but are not yet able to prove) that this could reflect the ability of the compound to inhibit a low affinity ‘off-target’ such as Aurora A, when binding to the higher affinity target protein PLK4 is compromised.

The centrinone-modulated phosphoproteome

Of the ~ 7500 ‘class I’ phosphosites (PTM-score ≥ 0.75) identified in clonal WT PLK4 cells (Figure 2E,F), 183 ($\sim 2.4\%$) were on peptides that were differentially regulated by centrinone using an adjusted p -value ≤ 0.05 (Supplementary Table S2). Of these, 130 phosphorylation sites were localised with $\geq 99\%$ site localisation confidence, i.e. PTM-score ≥ 0.994 [60]. The vast majority of the statistically differentially regulated phosphopeptides (containing 135 ‘class I’ phosphosites, 98 of which were localised at a 1% FLR) were down-regulated, consistent with inhibition of at least one protein kinase, or activation of at least one protein phosphatase. Using a slightly less stringent adjusted p -value ≤ 0.075 (where all p -values were ≤ 0.005), 468 ($\sim 6\%$) phosphopeptides containing 480 phosphosites (348 at 1% FLR) were differentially regulated by centrinone exposure, 318 of which were reduced, and might be considered to be potential PLK4 substrates.

To understand how many of these regulated phosphosites were considered to be previously ‘known’, we mapped them against data from large scale data repositories: PeptideAtlas (PA) phosphopeptide builds, and PhosphoSitePlus (PSP), categorising data from the different sources according to the strength of evidence (see Materials and methods). From this analysis, 99% of our identified ‘class I’ sites were considered high or medium confidence sites within PSP, and 94% considered high or medium confidence sites in PA. These comparisons both support our findings that these sites have been correctly localised in the vast majority of cases, and confirm previous identifications. Randomly incorrectly localised sites would generally occur with low confidence or fail to have supporting evidence from PSP and/or PA.

We also calculated the evolutionary conservation of the phosphosites across 100 model proteomes (50 mammals, 12 birds, 5 fish, 4 reptiles, 2 amphibians, 11 insects, 4 fungi, 7 plants, 5 protists; Supplementary Table S2), demonstrating that most of the sites are conserved in at least half of the proteomes, allowing for

conservative S/T substitutions (median 51%, upper quartile 68%; lower 44%). In the vast majority of cases, there are examples of conservation across mammals, birds, reptiles and fish, suggesting that these phosphorylation sites may contribute broadly to metazoan signalling pathways. Several sites, including Ser192 on Cdc42 effector protein 1 (down-regulated 1.6 fold in response to centrinone; p -value = 1.8×10^{-03}) and Ser48 in histone H4 (down-regulated 1.3-fold, p -value = 1.60×10^{-03}) are ~100% conserved across all eukaryotes tested (Supplementary Table S2).

Three differentially regulated phosphorylation sites were identified on PLK4 itself: Ser421, Ser665 and Ser821 (which are conserved in 55%, 44% and 43%, respectively, of 94 aligned species) all increased in response to centrinone treatment (Supplementary Figure S6, Supplementary Table S2). While the fold change for Ser421 matched the change in PLK4 protein level expression (both were up-regulated 1.8-fold), indicating no overall change in phosphorylation stoichiometry at this site, levels of pSer665 and pSer821 (2.3- and 3.7-fold, respectively) were notably higher in the presence of centrinone, suggesting modulation of these two sites by a regulated kinase or phosphatase. Although both Ser665 and Ser821 have previously been demonstrated to be phosphorylated in high-throughput MS-based studies [78], their functional roles remain to be defined. We did not find any evidence for changes in canonical multi-phosphodegron sites of phosphorylation in PLK4, likely due to the rapid turnover of PLK4 that occurs after phosphorylation at these sites.

Gene ontology (GO) analysis using DAVID also revealed that centrinone-regulated phosphorylation sites (adj. p -value ≤ 0.075) were significantly enriched in proteins involved in chromatin (up-regulated) and cadherin binding (down-regulated) (Figure 2G; Supplementary Figure S4). Interestingly, phosphoproteins in the nucleoplasm were also up-regulated, while levels of cytoplasmic proteins were reduced in a centrinone-dependent manner. In total, 22 centrosome phosphoproteins were significantly regulated, with the levels of 8 phosphoproteins increasing and 14 being reduced, including NUMA1 (pSer1769, pSer1991), LZTS2 (pSer311), RANBP1 (pSer60), XRCC4 (pSer256) and WDR62 (pSer33), a target of the physiological PLK4 targets CEP152 and CEP192 [11,12,37,79–81]. Phosphorylation sites on five members of the MAPK signalling pathway were also statistically differentially regulated: pThr693 on EGFR (p -value = 5.0×10^{-04} , adj. p -value = 5.0×10^{-02}) and pTyr204 on ERK1 (p -value = 3.4×10^{-03} , adj. p -value = 6.8×10^{-02}) were both up-regulated 1.5-fold, while pSer1275 on SOS1 (1.6-fold down-regulated, p -value = 1.1×10^{-03} , adj. p -value = 5.2×10^{-02}), pSer23 on MEK2 (MAP2K2; 1.5-fold, p -value = 1.2×10^{-04} , adj. p -value = 4.6×10^{-02}), and pSer62 on NMYC (2.1-fold, p -value = 1.4×10^{-03} , adj. p -value = 5.6×10^{-02}) were all down-regulated at least 1.5-fold. EGFR was the only one of these proteins to be differentially regulated at the protein level (1.2-fold up-regulation), although MAP3K2 (MEKK2), an upstream MAPK pathway regulator, was also down-regulated 1.2-fold at the protein level at an adj. p -value = 5.5×10^{-02} . Consequently, PLK4-dependent signalling is implicated in regulation of the MAPK pathway, which in turn can control entry into the cell cycle, amongst other functions. Consistent with this, and with the protein level changes discussed above, we observed centrinone-mediated regulation of many phosphopeptides from proteins implicated in cell cycle processes, including peptides containing: either (i) pSer277/pSer283 or (ii) pSer283/pSer285 from CDK11B (both down 1.3-fold); (iii) pSer332/pSer334 (1.2-fold up), (iv) pSer644 (1.3-fold down), (v) pSer681/pSer685 (1.5-fold down) on CDK12; (vi) pSer130 on CDK18 (1.2-fold down); (vii) pSer37 (1.4-fold down) and (viii) pThr821/826 (1.5-fold up) on RB1; (ix) pSer271 on cyclin D2 (2-fold down); (x) pSer387 on cyclin E1 (1.3-fold down). Interestingly, pSer74 on CDC6 was also reduced 1.3-fold in the presence of centrinone. CDC6 and PLK4 work antagonistically to regulate centriole duplication; this is driven by PLK4-mediated disruption of the CDC6-Sas-6 complex, and thus the ability of Sas-6 to interact with the centriole duplication core protein STIL. PLK4 binds directly to the N-terminal region of CDC6 in S-phase, disrupting the CDC6 Sas-6 interaction following CDC6 phosphorylation. Based on prediction and mutational analysis, PLK4 was previously shown to phosphorylate CDC6 *in vitro* on Ser30 and Thr527 [82]. Based on our data, we suggest that Ser74, which is conserved in ~70% of aligned eukaryotic orthologues, is a potential additional phosphosite on CDC6 that lies in a SerPro consensus downstream of centrinone in cells [82]. In agreement with the hypothesis that this is a direct PLK4 target, this phosphopeptide was not observed as differentially regulated in the G95R PLK4 cell line when treated with centrinone.

From the limited selection of physiological PLK4 substrates identified to date [38], we did not identify any known phosphopeptides that were statistically down-regulated in response to centrinone, likely due to our experimental procedure, in which cells were not chemically synchronised in S-phase despite centrinone-induced PLK4 stabilisation. Surprisingly, we observed a greater than 4-fold increase in levels of the phosphopeptide containing pSer237 (with respect to protein level changes) of BTRC (F-box/WD repeat-containing protein 1A), which has been previously reported to be associated with the PLK4 activator STIL [83], and 1.3-fold up-regulation of pSer3467 on the E3 ubiquitin-protein ligase MYCBP2.

Chemical-genetic PLK4 strategies have previously reported decreased phosphorylation of multiple proteins, including RUNX1, PTPN12, IL6ST, TRIM3 and SCRIB after conditional PLK4 knockdown or transgenic expression and inhibition of ‘analogue-sensitive’ PLK4 [13,35,38,84]. Many of these proteins have been assumed to be indirect targets of PLK4, due to the fact that they are not known to localise to the centrioles (or play known roles in centrosome or cilia biology). In our datasets, we also identified many confidently localised phosphosites for most of these proteins, notably Ser369 and Ser571 on PTPN12, a purported ERK site of phosphorylation [85], and Ser1309 and Ser1348 on SCRIB which were statistically down-regulated (q -value ≤ 0.075) after centrinone exposure, suggesting simplistically that they are likely to lie downstream of PLK4. Considering a reduced confidence threshold of statistical regulation (p -value < 0.05), Thr569 phosphorylation on PTPN12, as well as Ser708 and Ser1306 phosphorylation on SCRIB, were also found to be significantly down-regulated in our datasets. The use of drug-resistant kinase alleles can efficiently confirm on-target effects of small molecules [48,55,56]. However, in the case of drug-resistant G95R PLK4, Tet-induced cells behaved differently to WT-PLK4 in terms of effects on known PLK4 phosphorylation site motifs, meaning that we could not use experimental cellular evidence to validate on-target PLK4 phosphorylation with this system. Consequently, we resorted to biochemical methods.

Can PLK4 directly phosphorylate a Pro-rich amino acid consensus in proteins?

Motif analysis of the 318 phosphorylation sites on peptides that were down-regulated in response to centrinone (adj. p -value ≤ 0.075) revealed very strong enrichment for phosphorylation sites in a Pro-rich consensus, with a Pro residue prevalent at the +1 position (Figure 4A; Supplementary Table S2). Indeed, 219 (69%) of the unique (type I) phosphosites identified in cells were immediately followed by a Pro residue (Figure 4B), with 91 phosphorylation sites additionally containing Pro at +2 ([pS/pT]PP consensus), while 78 and 76 phosphosites contain a Pro at −1 or −2, respectively (P[pS/pT]P or Px[pS/pT]P). Although a canonical PLK4 peptide

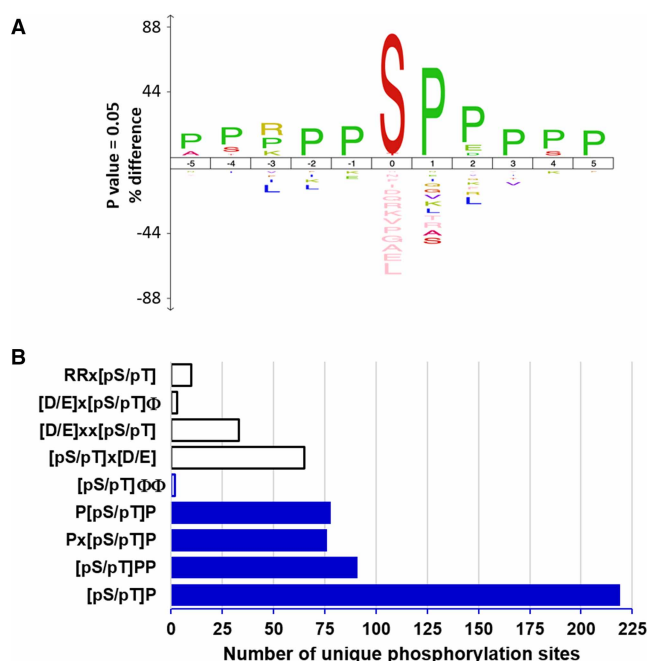


Figure 4. PLK4 phosphorylates serine and threonine residues in a proline consensus.

(A) Centrinone-down-regulated phosphorylation site sequence conservation using IceLogo [66] reveals extensive Pro enrichment around the site of phosphorylation. (B) Frequency of novel Pro-directed motifs (blue), the known consensus sequence for Aurora A (RR[pS/pT]), or the acidic residue-rich motifs of PLK1 ([D/E]x[pS/pT]Φ, where Φ represents hydrophobic Y/F/I/L/V residues and x is any amino acid), PLK2 ([D/E]xx[pS/pT]), PLK3 ([pS/pT]x[D/E]) or the classic hydrophobic PLK4 consensus ([pS/pT]ΦΦ) across all centrinone-down-regulated phosphorylation sites.

phosphorylation consensus motif has been described in which one or two hydrophobic (Φ) residues reside immediately C-terminal to the site of phosphorylation [47], only 2 (~1%) of the identified centrinone-down-regulated phosphorylated sites contained Y/F/I/L/V in both of these ‘canonical’ positions (Figure 4B). Even considering a single hydrophobic residue at either positions +1 or +2, the number of phosphosites within this motif was significantly lower at 52, than the number observed within a Pro-rich consensus (216, Figure 4B). Interestingly, 2 of the 16 autophosphorylation sites that we identified on recombinant PLK4 (Ser174 and Ser179) were also followed by a Pro residue (Supplementary Figure S1B), indicating that a Pro at this position is permissible for phosphorylation by PLK4. In considering potential off-target effects of centrinone on either Aurora A or other PLK family members, we also interrogated the down-regulated phosphorylation sites for the RRx[S/T] Aurora A consensus and the classic [D/E]x[S/T] Φ consensus of PLK1 [42]. However, only 10 centrinone inhibited sites were observed that contained a basic Arg residue at both –1 and –2, and only three sites fitted the PLK1 substrate consensus (Figure 4B). In agreement with these observations, we also determined that a significant proportion (47%) of the 141 phosphopeptides down-regulated in a recent study evaluating PLK4 substrates using analogue-sensitive alleles in human RPE-1 cells [38] also contained a Pro at +1 relative to the site of modification, compared with only 15% that possess a hydrophobic residue at +1 and/or +2 from the site of phosphorylation.

To experimentally validate centrinone-regulated sites identified as potential PLK4 substrates in cells, and to examine our hypothesis of a potential Pro-driven consensus motif for this kinase, several recombinant proteins were evaluated for their ability to be phosphorylated by active PLK4 *in vitro*. Both NMYC and PTPN12 contained phosphorylation sites with a Pro at +1 that were statistically down-regulated following cellular exposure to centrinone: pSer62 on NMYC (2.1-fold, p -value = 1.4×10^{-03} , adj. p -value = 5.6×10^{-02} , conserved in 71% of aligned species), a site previously reported to be phosphorylated by cyclin B/Cdk1 in prophase [86], and two sites on PTPN12: pSer369 (1.3-fold, p -value = 2.4×10^{-03} , adj. p -value = 6.4×10^{-02} , conserved in 89% of species) and pSer571 (1.3-fold, p -value = 2.4×10^{-03} , adj. p -value = 6.4×10^{-02} , conserved in 60%), a site previously shown to be phosphorylated by ERK1/2 *in vitro* [85]. Interestingly, both PTPN12 phosphosites also contained a Pro at –1 as well as a Pro at +1. NMYC and PTPN12 were thus selected as potential PLK4 substrates for biochemical analysis.

PLK4 kinase assays employing either recombinant NMYC or PTPN12 as substrates readily confirmed efficient (similar to PLK4 autophosphorylation) phosphorylation of both proteins *in vitro* (Figure 5 and 6;

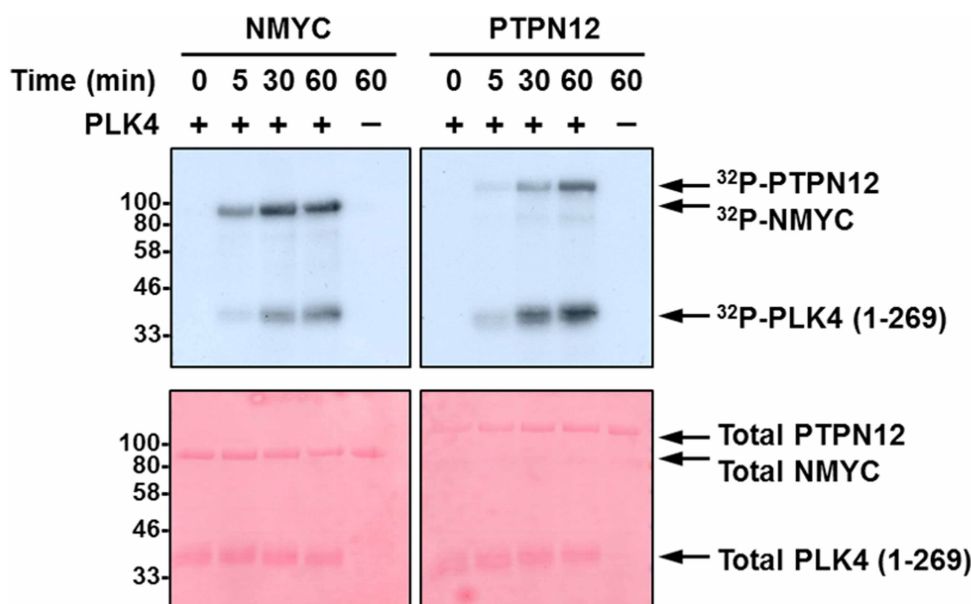


Figure 5. PLK4 phosphorylates NMYC and PTPN12 *in vitro*.

Autoradiogram (top) or Ponceau stained membrane (bottom) following *in vitro* ^{32}P -based phosphorylation of either recombinant NMYC or PTPN12 by recombinant PLK4 catalytic domain.

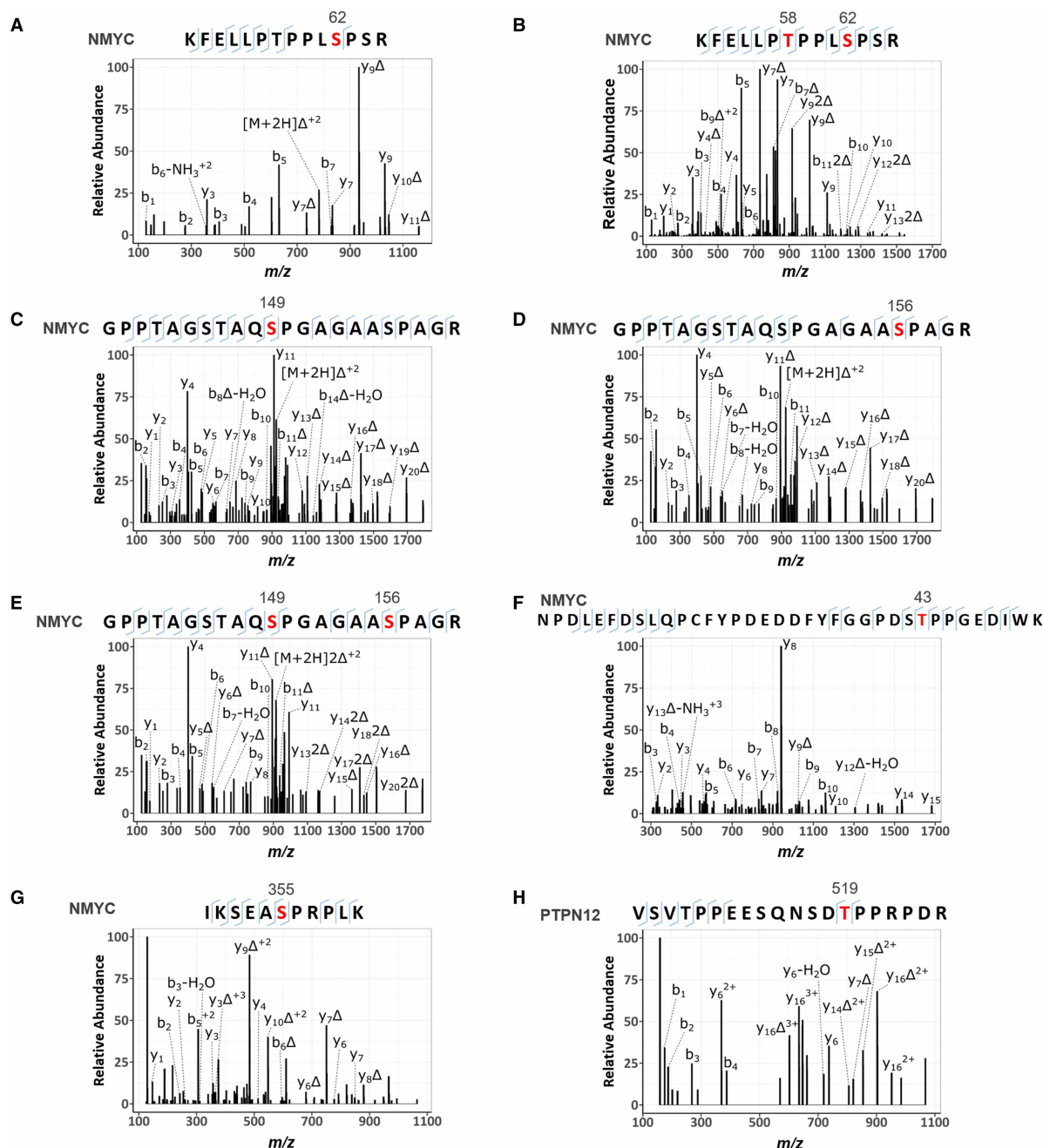


Figure 6. HCD product ion mass spectra of PLK4-dependent [pS/pT]P phosphorylated tryptic peptides from NMYC and PTPN12.

Recombinant NMYC (**A–G**) and PTPN12 (**H**) proteins were incubated in 50 mM Tris–HCl, pH 7.4, 100 mM NaCl, 1 mM DTT, 1 mM ATP and 5 mM MgCl₂ at 30°C in the absence and presence of PLK4. Reactions were then digested with trypsin and subjected to TiO₂-based phosphopeptide enrichment and LC–MS/MS analysis, as described in Materials and methods. (**A**) Doubly charged ion at *m/z* 831.4367 indicates phosphorylation of NMYC at Ser62; (**B**) triply charged ion at *m/z* 581.2839 indicates phosphorylation of NMYC at Thr58 and Ser62; (**C,D**) doubly charged ion at *m/z* 973.4420 indicated phosphorylation of NMYC at either Ser149 (**C**) or Ser156 (**D**); (**E**) triply charged ion at *m/z* 675.9525 indicated phosphorylation of NMYC at Ser149 and Ser156; (**F**) triply charged ion at *m/z* 1430.5940, indicated phosphorylation of NMYC at Thr43; (**G**) triply charged ion at *m/z* 435.9026 indicates phosphorylation of NMYC at Ser355; (**H**) triply charged ion at *m/z* 763.3448 indicates phosphorylation of PTPN12 at Thr519. Red denotes the site of phosphorylation. Δ equates to loss of H₃PO₄.

Table 2). MS-based phosphorylation site mapping of recombinant NMYC with catalytically active recombinant PLK4 confirmed Ser26(Pro) as a PLK4-dependent phosphorylation site (Table 2; Figure 6). Many additional PLK4-dependent phosphosites were also identified, including Thr43, Thr58, Ser131, Ser149, Ser156, Ser315, Ser355 and Ser400, five of which (underlined) also possess a Pro at the +1 position. Interestingly, this region of NMYC contains an extended Aurora A docking site in the N-terminus [87], which also hosts a phosphodegrogen centred around Pro-directed Thr58, whose phosphorylation via GSK3 and a Pro-directed kinase has been shown to be required for recognition by the E3 ubiquitin ligase SCF^{FbxW7} [88,89]. In a separate experiment, full-length recombinant PTPN12 was also phosphorylated by PLK4 *in vitro* on four residues (Ser435, Ser499, Thr519, Ser606), including notably Thr519, which lies in a pTPP consensus (Table 2, Figure 6). Ser369 and Ser571, which changed in cells in the presence of centrinone, were not identified under these conditions (Table 2).

Analysis of peptide phosphorylation by recombinant PLK4

To further evaluate the hypothesis that PLK4 might function as a Pro-directed kinase, we undertook a series of peptide-based kinase assays beginning with our standard PLK4 peptide substrate, FLAKSFGSPNRAYKK, which is derived from the activation segment of CDK7/CAK [27]. This peptide contains two potential sites of Ser/Thr phosphorylation, including one Ser-Pro site. The precise site of PLK4-dependent phosphorylation in this peptide substrate has not previously been defined. Based on the quantitative phosphoproteomics data, and the protein assays described above, we hypothesised that PLK4 directly catalyses phosphorylation of Ser8 in this peptide, since this phosphoacceptor residue is immediately followed by Pro.

However, MS-based phosphosite mapping revealed that the incorporated phosphate quantified by microfluidic phosphopeptide mobility assay (Figure 7A) resides solely on Ser5, as opposed to Ser8, of this peptide (Supplementary Figure S7). Phosphorylation of Ser5 was then confirmed (indirectly) by using a variant peptide

Table 2. MS-based analysis of NMYC and PTPN12 phosphorylation sites

Protein	Peptide sequence	Phosphorylation site	Novel?	In vitro (PLK4)		In cellulo		
				Mascot score	ptmRS score	Andromeda score	PTM-score	Fold change
N-myc	NPDLFSDLPQCFYPDEDDFYFGGPDSTPPGEDIWK	Thr43	Yes	29	99.45		N.O.	
	KFELLPTPLSPSR	Thr58/Ser62	No (5/4 LTP, 38/32 HTP)	37	100/100	85.9	1.00/0.88	N.S.
	KFELLPTPLSPSR	Ser62	No (4 LTP, 32 HTP)	26	99.75	154.6	0.98	2.1 down
	AVSEKIQHGR	Ser131	Yes	24	100		N.O.	
	GPPTAGSTAQSPGAGAAAPAGR	Ser149	Yes	129	100		N.O.	
	GPPTAGSTAQSPGAGAAAPAGR	Ser156	No (4 HTP)	88	100		N.O.	
	GPPTAGSTAQSPGAGAAAPAGR	Ser149/Ser156	Yes/No	62	100/100		N.O.	
	AQSEELIKR	Ser315	Yes	48	100		N.O.	
	IKSEAAPRPLK	Ser355	No (3 HTP)	41	100		N.O.	
	SSFLTLR	Ser400	Yes	46	99.83		N.O.	
PTPN12	IADGVNEINTENMVSSIEPEKQDPPPKPPR	Ser332	No (29 HTP)		N.O.	276.7	1.00	N.S.
	EEILQPPPEHPVPILTPSPPSAFTVTTVWQDNDNR	Ser369	No (3 HTP)		N.O.	122.5	0.92	1.3 down
	NLSFEIK	Ser435	No (2 LTP, 96 HTP)	36	100	109.9	1.00	1.3 up
	SFDGNTLLNR	Ser449	No (32 HTP)		N.O.	256.7	1.00	1.6 up
	ISKPOELSSDLNVGDTSCNVDCSVTQSNK	Ser499	Yes	74	99.69		N.O.	
	VSVTPPEESQNSDTPPRPDR	Thr509	No (27 HTP)		N.O.	114.6	1.00	N.S.
	VSVTPPEESQNSDTPPRPDR	Thr519	No (20 HTP)	29	99.23		N.O.	
	TVSLTPSPPTQVETPDVLDHNDTSPLFR	Ser569/Ser571	No (1 LTP, 9/14 HTP)		N.O.	142.4	0.99/0.86	1.4 down
	TVSLTPSPPTQVETPDVLDHNDTSPLFR	Ser571	No (1 LTP, 14 HTP)		N.O.	218.7	1.00	1.3 down
	TPLSFTNPLHSDSDSDER	Ser603/Ser606	No (34/33 HTP)		N.O.	192.1	1.00/0.98	N.S.
	TPLSFTNPLHSDSDSDER	Ser606	No (33 HTP)	38	99.82		N.O.	
	DVDVSEDSPPLPER	Ser673	No (52 HTP)		N.O.	252.2	1.00	N.S.

Phosphopeptides identified from NMYC or PTPN12 by MS/MS following either *in vitro* phosphorylation by PLK4, or from human cells. The phosphopeptide sequences and the identified site(s) of phosphorylation (underlined within the sequence) are indicated, as well as their Mascot and ptmRS scores (*in vitro*), or Andromeda and PTM-score (from the cellular analysis), indicating site localisation confidence. Fold-change details the quantitative effect on phosphopeptide levels in response to centrinone. 'Novelty' indicates whether these identified phosphosites were previously recorded in PhosphoSitePlus, and whether these records were annotated as either low-throughput (LTP) or high-throughput (HTP) observations. N.O. – not observed; N.S. no-significant change in response to centrinone.

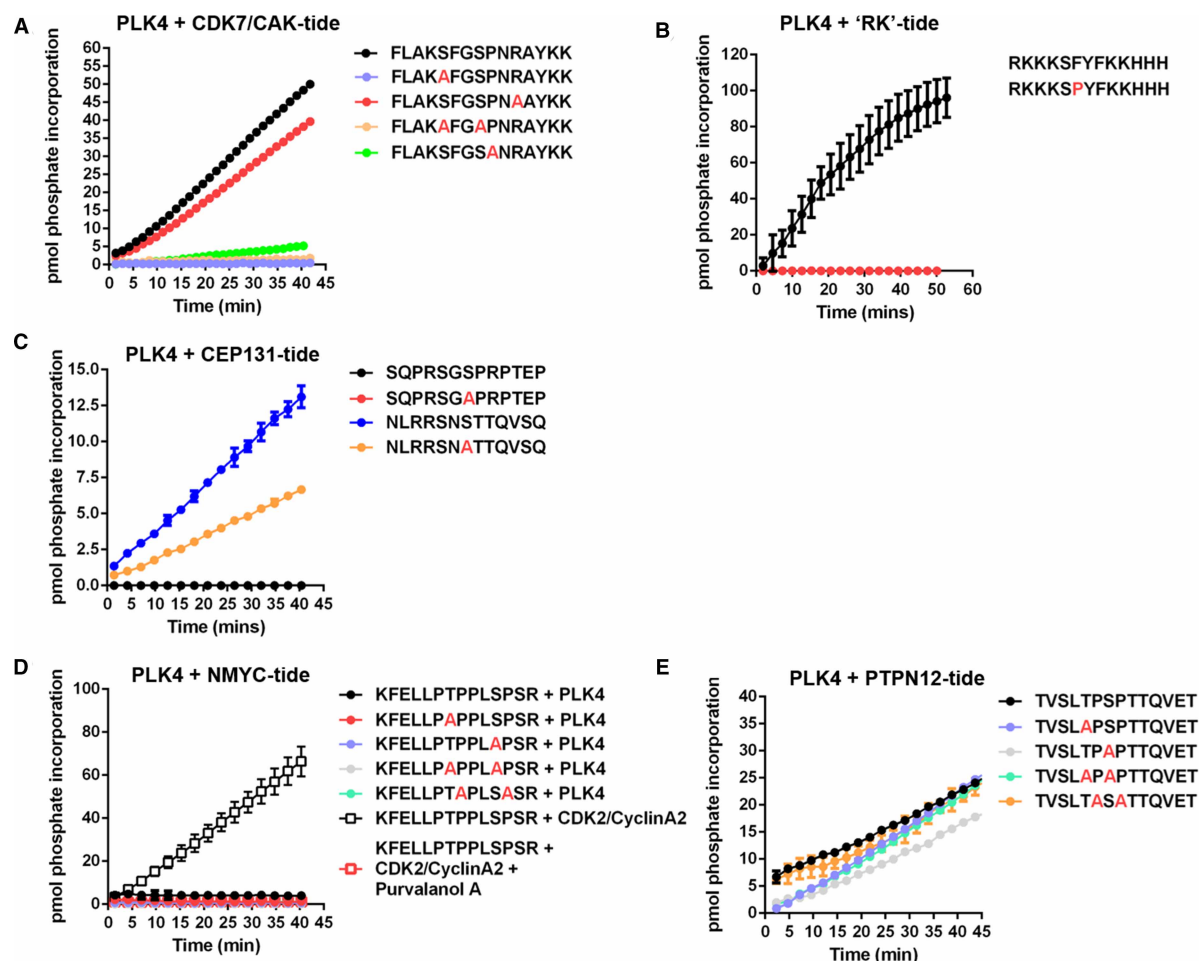


Figure 7. PLK4 substrate specificity differs towards peptide substrates.

PLK4 or CDK2/CyclinA2 activity was quantified in a time-dependent manner using the indicated fluorescently labelled synthetic peptide substrates: (A) CDK7/CAK derived substrates; (B) 'RK' and 'RK' F6P substrate; (C) CEP131 derived substrates; (D) NMYC derived substrates; (E) PTPN12 derived substrates. All assays were performed at room temperature (20°C) using 2 μ M final concentration of the appropriate peptide substrate, 1 mM ATP and 500 ng PLK4 or 10 ng CDK2/CyclinA2 as indicated. The specific activity (pmol phosphate incorporation) was calculated from integrated phospho:dephosphopeptide ratios at the indicated time points after assay initiation.

where Ser5 was replaced with Ala (S5A), which was not phosphorylated by PLK4 (Figure 7A). Interestingly, the single mutation of Pro9 to Ala also greatly reduced phosphorylation at Ser5, through an unknown mechanism that presumably involves peptide recognition to prime Ser5 phosphorylation. To supplement this analysis, a different PLK4 peptide substrate lacking a Pro residue was synthesised for mobility-based kinase assays based on the published canonical [pS/pT] $\Phi\Phi$ PLK4 phosphorylation consensus motif, (RKKKSFYFKKHHH) termed 'RK' [47]. This peptide was also exploited to evaluate the effects of a Pro at +1 by single amino acid replacement (RKKKSYPYFKKHHH). The substrate was phosphorylated more efficiently by PLK4 than our standard peptide (Figure 7B), but replacement of Phe at +1 with a Pro residue completely abolished PLK4-dependent phosphorylation, as previously reported in high-throughput studies [47]. Thus, although Pro at +1 is permissible for direct PLK4 phosphorylation in some protein substrates (Figure 1, Table 2, Figure 6), synthetic peptide data demonstrate that Pro at the +1 position is not tolerated when short peptide motifs are presented as potential substrates, despite evidence for phosphorylation in intact proteins containing these same sequences.

Next, we turned our attention to PLK4 substrates derived from known cellular substrates, including those lying downstream of centrinone. Initially, we evaluated two (overlapping) peptides derived from phosphorylated CEP131, a centriolar PLK4 substrate [38]. We confirmed that a CEP131 peptide containing the sequence

surrounding Ser78 (embedded in NSTT), but not a peptide containing the sequence surrounding Ser89 (embedded in GSPRP), were phosphorylated in real-time by PLK4. The substitution of Ser78 for Ala reduced phosphorylation by ~50%, suggesting additional peptide modification site(s) in this peptide (Figure 7C). We also evaluated a peptide substrate designed around the Thr58/Ser62 [pS/pT]P phosphorylation sites that we identified in NMYC, which are centrinone-dependent events in cells (pSer62; Supplementary Table S2) and PLK4 phosphorylation sites in NMYC protein *in vitro* (Figure 6B; Table 2). Surprisingly, none of the synthetic short NMYC peptides were detectably phosphorylated by PLK4 (Figure 7D). However, to confirm the ability of this peptide to function as a kinase substrate we showed that it was phosphorylated by the Pro-directed kinase CDK2/cyclinA2 in a Purvalanol-dependent manner (Figure 7D). Finally, although a peptide designed around the cellular pT569/pS571 phosphosites identified in PTPN12 (which are centrinone-responsive) was a substrate for PLK4, this was largely independent of a Pro residue at the +1 position at either of these residues, based on similar rates of phosphorylation after mutation of either or both of these phosphorylatable residues to Ala (Figure 7E). This is in broad agreement with our *in vitro* protein data for PTPN12 (Table 2), where we found that although recombinant PTPN12 is a PLK4 substrate (including a single validated pTP consensus), centrinone-sensitive Pro-directed PTPN12 phosphorylation sites identified in cells were not detectably phosphorylated *in vitro*.

Discussion

In this study, we developed a quantitative phosphoproteomics approach to explore PLK4-mediated signalling in human cells and attempted to identify novel cellular PLK4 targets by exploiting the target-validated PLK4-selective inhibitor centrinone. Of the 480 phosphorylation sites identified on peptides that were differentially regulated in FLAG-WT PLK4 U2OS cells exposed to centrinone (at an adjusted *p*-value ≤ 0.075 , where all *p*-values were ≤ 0.005), 318 were found on peptides whose levels decreased in the presence of the compound, suggesting either direct (or indirect) regulation through inhibition of PLK4 catalytic activity. The majority of these sites are conserved across eukaryotes, suggesting evolutionarily conserved PLK4-mediated signalling mechanisms. Surprisingly, sequence analysis of the residues surrounding these down-regulated phosphorylation sites revealed a highly dominant Pro-rich phosphorylation consensus, notably at positions +1, -1/-2 with respect to the site of phosphorylation (Figure 4A). Indeed, ~70% of the phosphosites that were reduced in the presence of centrinone possessed a Pro at +1, with 42% of those also containing a Pro residue at +2 (Figure 4B).

As well as identifying many centrinone inhibited phosphorylation sites on multiple cell cycle-regulating proteins that might be PLK4 substrates (including CDK11, CDK12, CDK18, RB1, cyclin D2, cyclin E1 and CDC6), we report two new centrinone-regulated proteins as direct PLK4 substrates, NMYC and PTPN12, which we validate using *in vitro* kinase assays and MS-based site analysis (Figures 5 and 6). Of 13 PLK4-dependent phosphorylation sites mapped in NMYC and PTPN12 (9 and 4, respectively), 6 are followed by a Pro residue (Table 2, Figure 6), supporting the idea that in some protein substrates, PLK4 possesses an ability to function as a Pro-directed Ser/Thr kinase. Previous high-throughput studies agree with these findings, including the mapping of Pro-directed autophosphorylation sites on PLK4 [26,27], and *in vitro* MS-based site-mapping demonstrating PLK4 phosphorylation of Ser and Thr residues followed by a Pro residue in the physiological substrate STIL [16]. These findings contrast with other assays that employ synthetic substrates, including sequence consensus motifs identical with phosphorylation sites mapped in cellular PLK4 targets [38,46,47] (Figure 6, Table 2 and Supplementary Table S2). We thus hypothesise that under some conditions, PLK4 has the ability to phosphorylate [pS/pT]P motifs in a manner that is dependent on long-range interactions within its protein substrates. For example, these could involve phosphorylated Polo box-binding sequences deposited on PLK4 substrates by PLK4 itself, or by a variety of ‘priming’ kinases. Whatever the mechanisms at play, our data suggest that comparison of substrate recognition sequences from peptide-based screening should be used with some caution when evaluating cellular proteomics data to understand kinase substrate relationships. Indeed, in the case of previous phosphoproteomics datasets obtained with analogue-sensitive PLK4 and PP1 analogues, or through *in vitro* mapping of physiological substrates such as Ana2/STIL, multiple [pS/pT]P sites have been deposited in databases, but appear to have been largely ignored. As a specific example, of 84 STIL phosphorylation sites directly phosphorylated by PLK4 *in vitro*, 14 reside in either a pSP or pTP consensus [16]. Moreover, the phosphorylation of putative PLK4 substrates, including RUNX1, TRIM3, SCRIB and CEP131 on [S/T]P sites [38,90], have been reported, and many of these PLK4-phosphorylated [pS/pT]P motifs are conserved in eukaryotes.

Although we validate NMYC and PTPN12 as new PLK4 substrates, we cannot rule out that some of the (Pro and indeed non Pro-directed) centrinone inhibited phosphorylation sites found in the cellular proteome are either (i) off-target to centrinone, or (ii) indirect effects of PLK4 inhibition of a downstream Pro-directed kinase, perhaps one that is involved in ‘priming’ PLK4 binding via one of the PLK4 PBDs. In an attempt to mitigate against such off-target effects of centrinone, we exploited cell lines expressing G95R PLK4 that is predicted to be unable to bind the inhibitor, and remains catalytically viable (Supplementary Figure S1). However, based on the results reported here, we predict that interpretation of the quantitative phosphoproteomics data with this cell line are confounded by centrinone-mediated inhibition of both the endogenous PLK4 protein, which is still present at low levels in these studies, and ‘off-targets’ of the compound. In considering cellular targets of centrinone, including potential off-targets of the VX-680 parental compound, such as Aurora A and B, we also interrogated the sequence context of down-regulated phosphosites for the classical Aurora A/B (and PLK1/3) substrate motifs. Although phosphorylation sites were identified on down-regulated phosphopeptides that matched the basophilic consensus motifs for these kinases, when combined, these still only accounted for <25% of the ‘non-Pro’ directed motifs identified, suggesting that inhibition of these enzymes is not a major confounding issue for analysis of data obtained with this compound. The total depletion of endogenous PLK4 (e.g. by CRISPR/Cas9) strategies is challenging due to its fundamental role in cellular biology, thus it has not been possible for us to generate an inducible system in a ‘clean’ PLK4 null background. However, it will be of interest in future to engineer a G95R PLK4 germline mutation and then model specific ‘on’ and ‘off’ targets of centrinone more carefully under a series of defined experimental conditions.

We observed that many Pro-directed sites of phosphorylation are inhibited by centrinone. Our standard synthetic PLK4 substrate is derived from the activation segment of the CDK activating kinase CDK7, which it phosphorylates on Ser5 in the sequence ‘KSF’, just after the DFG motif (Table 1, Supplementary Figure S7). This finding raises the possibility that centrinone-mediated inhibition of PLK4 might directly reduce the activity of other downstream kinases with site specificities for distinct activation-segment motifs in cells. Potential targets to investigate in the future include CDK7 itself, CDK11, CDK12 and the DNA-damage response modulator CDK18 [91], which all possess centrinone-sensitive phosphorylation sites (Supplementary Figure S2), and whose substrate specificity (where known) conforms to the Pro-rich motif identified in other proteins found here. However, of the CDK phosphorylation sites that we observed to be modulated by centrinone, none lie within the catalytic (or other known regulatory) domains, and crucially, none are known to regulate protein kinase activity. CHK2 is the only previously defined *in vitro* substrate of PLK4 with protein kinase activity [92] found in our study. However, although it possesses a flexible substrate recognition motif, previous studies have suggested that a basophilic Arg at –3 is preferential for substrate phosphorylation [93], likely ruling out this enzyme as the intermediary of a centrinone-regulated PLK4 network that controls the [pS/pT]P consensus sites reported here. Indeed, the fact that we also identify direct [pS/pT]Pro sites as PLK4 protein targets *in vitro* significantly raises the likelihood that a proportion of the ~300 centrinone inhibited phosphosites identified in cells may well be direct targets of PLK4. The subcellular protein complexes involved in determining these modifications in human cells, and whether they occur co- or post-translationally, remain to be identified.

Multiple members of the CMGC kinase family possess well-documented Pro-directed substrate specificity. Although CDK complexes such as Cyclin B-CDK1 phosphorylate a plethora of crucial M-phase substrates, containing minimal [S/T]P and full consensus [S/T]PXX[L/R] motifs [94–97], it is now clear that at least one CDK enzyme complex can also phosphorylate non-[S/T]P consensus motifs [98], operating through a combined ‘multisite’ code [99], differential substrate co-localisation and ordered phosphorylation that is dependent on substrate affinity [100,101]. Similar findings have also been made with the abscission-controlling PKCε-Aurora B complex, whose substrate specificity can switch at different phases of the cell cycle [102]. In the context of PLK4, further studies with full-length proteins are justified to examine whether PLK4 substrate specificity might be altered depending upon the subcellular repertoire of regulatory proteins/substrates formed. Moreover, we speculate that PLK4 substrate-targeting PBDs 1–3 (which are absent from our biochemical analysis, but present in cellular experiments) are worthy of further investigation in order to evaluate differences established for PLK4 protein and peptide substrate specificities, either after immunoprecipitation of PLK4 interactomes from cells, or in reconstituted biochemical assays.

Conclusions

In this study, we show that exposure of human cells to the PLK4 inhibitor centrinone generates unexpected diverse effects on the phosphoproteome. Our data suggest that the centrinone target PLK4, or a distinct

PLK4-regulated kinase(s), phosphorylates [S/T]P motifs on multiple cellular proteins. Notably, protein phosphorylation in this broad [pS/pT]P consensus is markedly down-regulated in human cells exposed to centrinone, and PLK4 is able to phosphorylate residues with a Pro at +1 in recombinant proteins (but not derived synthetic peptides) that includes two new PLK4 substrates, PTPN12 and NMYC. In the future, the biological effects of these phosphorylation events will be explored further, in the context of catalytic output of the tyrosine phosphatase PTPN12 and the potential for PLK4 integration into the Aurora A/FBX7/NMYC signalling network. It is anticipated that when assessed alongside complementary PLK4 chemical genetic, depletion or elimination strategies, our proteomic datasets will help define further physiological PLK4 substrates across the cell cycle. These findings will also allow the extent to which a [pS/pT]P phosphorylation consensus represents a direct, indirect or substrate-dependent PLK4 modification in cells, and thus permit the biological roles of PLK4 to be examined in more detail.

Data availability

All data needed to evaluate the conclusions made are available in the main or supplementary sections of the paper. The mass spectrometry proteomics data have been deposited to the ProteomeXchange Consortium via the PRIDE partner repository [103] with the dataset identifier PXD018704 and 10.6019/PXD018704.

Open access

Open access for this article was enabled by the participation of University of Liverpool in an all-inclusive Read & Publish pilot with Portland Press and the Biochemical Society under a transformative agreement with JISC.

Competing Interests

The authors declare that there are no competing interests associated with the manuscript.

Funding

This work was funded by a North West Cancer Research (NWCR) grants CR1097 and CR1208 (to DPB and PAE), CR1157 and CR1088 (to CEE and PAE), the Biotechnology and Biological Sciences Research Council (BBSRC; BB/R000182/1 and BB/M012557/1 to CEE) and Cancer Research UK (C1443/A22095 to CEE).

Author Contributions

D.P.B., P.A.E. and C.E.E. obtained funding, designed the experiments and analysed the data alongside C.J.C. and A.C. A.K., S.P. and A.R.J. performed bioinformatics analysis. C.J.C., A.C. and P.J.B. performed MS analysis, and D.M. and staff in the Centre for Cell Imaging helped with immunofluorescence studies. P.A.E. and C.E.E. wrote the paper, with contributions from all authors, who also approved the final version prior to submission.

Acknowledgements

We thank Dr Gopal Sapkota (University of Dundee) for the generous donation of parental U2OS cells. The authors also wish to thank Prof. Sonia Rocha for help with FACS analysis, Sam Evans for media preparation, Alex Holme for technical support, and the Centre for Cell Imaging at the University of Liverpool.

Abbreviations

ATP, adenosine 5'-triphosphate; DMSO, dimethyl sulfoxide; MS, mass spectrometry; MS/MS, tandem mass spectrometry; NMYC, N-myc proto-oncogene protein; PBD, polo box domain; PLK, Polo-like kinase; PTPN12, protein tyrosine phosphatase non-receptor type 12.

References

- 1 Bettencourt-Dias, M., Rodrigues-Martins, A., Carpenter, L., Riparbelli, M., Lehmann, L., Gatt, M.K., et al. (2005) SAK/PLK4 is required for centriole duplication and flagella development. *Curr. Biol.* **15**, 2199–2207 <https://doi.org/doi:10.1016/j.cub.2005.11.042>
- 2 Habedanck, R., Stierhof, Y.D., Wilkinson, C.J. and Nigg, E.A. (2005) The Polo kinase Plk4 functions in centriole duplication. *Nat. Cell Biol.* **7**, 1140–1146 <https://doi.org/doi:10.1038/ncb1320>
- 3 Breslow, D.K. and Holland, A.J. (2019) Mechanism and regulation of centriole and cilium biogenesis. *Annu. Rev. Biochem.* **88**, 691–724 <https://doi.org/doi:10.1146/annurev-biochem-013118-111153>
- 4 Lopes, C.A., Jana, S.C., Cunha-Ferreira, I., Zitouni, S., Bento, I., Duarte, P., et al. (2015) PLK4 trans-autoactivation controls centriole biogenesis in space. *Dev. Cell* **35**, 222–235 <https://doi.org/doi:10.1016/j.devcel.2015.09.020>

- 5 Peel, N., Dougherty, M., Goeres, J., Liu, Y. and O'Connell, K.F. (2012) The *C. elegans* F-box proteins LIN-23 and SEL-10 antagonize centrosome duplication by regulating ZYG-1 levels. *J. Cell Sci.* **125**, 3535–3544 <https://doi.org/doi:10.1242/jcs.097105>
- 6 Holland, A.J., Lan, W., Niessen, S., Hoover, H. and Cleveland, D.W. (2010) Polo-like kinase 4 kinase activity limits centrosome overduplication by autoregulating its own stability. *J. Cell Biol.* **188**, 191–198 <https://doi.org/doi:10.1083/jcb.200911102>
- 7 Kleylein-Sohn, J., Westendorf, J., Le Clech, M., Habedanck, R., Stierhof, Y.D. and Nigg, E.A. (2007) Plk4-induced centriole biogenesis in human cells. *Dev. Cell* **13**, 190–202 <https://doi.org/doi:10.1016/j.devcel.2007.07.002>
- 8 Rodrigues-Martins, A., Riparbelli, M., Callaini, G., Glover, D.M. and Bettencourt-Dias, M. (2007) Revisiting the role of the mother centriole in centriole biogenesis. *Science* **316**, 1046–1050 <https://doi.org/doi:10.1126/science.1142950>
- 9 Dzhindzhev, N.S., Tzolovsky, G., Lipinski, Z., Abdelaziz, M., Debski, J., Dadlez, M., et al. (2017) Two-step phosphorylation of Ana2 by Plk4 is required for the sequential loading of Ana2 and Sas6 to initiate procentriole formation. *Open Biol.* **7**, 170247 <https://doi.org/doi:10.1098/rsob.170247>
- 10 Ohta, M., Ashikawa, T., Nozaki, Y., Kozuka-Hata, H., Goto, H., Inagaki, M., et al. (2014) Direct interaction of Plk4 with STIL ensures formation of a single procentriole per parental centriole. *Nat. Commun.* **5**, 5267 <https://doi.org/doi:10.1038/ncomms5267>
- 11 Kim, T.S., Park, J.E., Shukla, A., Choi, S., Murugan, R.N., Lee, J.H., et al. (2013) Hierarchical recruitment of Plk4 and regulation of centriole biogenesis by two centrosomal scaffolds, Cep192 and Cep152. *Proc. Natl Acad. Sci. U.S.A.* **110**, E4849–E4857 <https://doi.org/doi:10.1073/pnas.1319656110>
- 12 Arquint, C., Sonnen, K.F., Stierhof, Y.D. and Nigg, E.A. (2012) Cell-cycle-regulated expression of STIL controls centriole number in human cells. *J. Cell Sci.* **125**, 1342–1352 <https://doi.org/doi:10.1242/jcs.099887>
- 13 Moyer, T.C., Clutario, K.M., Lambrus, B.G., Daggubati, V. and Holland, A.J. (2015) Binding of STIL to Plk4 activates kinase activity to promote centriole assembly. *J. Cell Biol.* **209**, 863–878 <https://doi.org/doi:10.1083/jcb.201502088>
- 14 Kratz, A.S., Barenz, F., Richter, K.T. and Hoffmann, I. (2015) Plk4-dependent phosphorylation of STIL is required for centriole duplication. *Biol. Open* **4**, 370–377 <https://doi.org/doi:10.1242/bio.201411023>
- 15 Dzhindzhev, N.S., Tzolovsky, G., Lipinski, Z., Schneider, S., Lattao, R., Fu, J., et al. (2014) Plk4 phosphorylates Ana2 to trigger Sas6 recruitment and procentriole formation. *Curr. Biol.* **24**, 2526–2532 <https://doi.org/doi:10.1016/j.cub.2014.08.061>
- 16 Moyer, T.C. and Holland, A.J. (2019) PLK4 promotes centriole duplication by phosphorylating STIL to link the procentriole cartwheel to the microtubule wall. *eLife* **8**, e46054 <https://doi.org/doi:10.7554/eLife.46054>
- 17 Tian, X., Zhou, D., Chen, L., Tian, Y., Zhong, B., Cao, Y., et al. (2018) Polo-like kinase 4 mediates epithelial-mesenchymal transition in neuroblastoma via PI3K/Akt signaling pathway. *Cell Death Dis.* **9**, 54 <https://doi.org/doi:10.1038/s41419-017-0088-2>
- 18 Kazazian, K., Go, C., Wu, H., Brashavitskaya, O., Xu, R., Dennis, J.W., et al. (2017) Plk4 promotes cancer invasion and metastasis through Arp2/3 complex regulation of the actin cytoskeleton. *Cancer Res.* **77**, 434–447 <https://doi.org/doi:10.1158/0008-5472.CAN-16-2060>
- 19 Rosario, C.O., Kazazian, K., Zih, F.S., Brashavitskaya, O., Haffani, Y., Xu, R.S., et al. (2015) A novel role for Plk4 in regulating cell spreading and motility. *Oncogene* **34**, 3441–3451 <https://doi.org/doi:10.1038/nc.2014.275>
- 20 Liu, Y., Kim, J., Philip, R., Sridhar, V., Chandrasekhar, M., Moffat, J., et al. (2020) Direct interaction between CEP85 and STIL mediates Plk4-driven directed cell migration. *J. Cell Sci.* **133**, jcs238352 <https://doi.org/doi:10.1242/jcs.238352>
- 21 Luo, Y., Barrios-Rodiles, M., Gupta, G.D., Zhang, Y.Y., Ogunjimi, A.A., Bashkurov, M., et al. (2019) Atypical function of a centrosomal module in WNT signalling drives contextual cancer cell motility. *Nat. Commun.* **10**, 2356 <https://doi.org/doi:10.1038/s41467-019-10241-w>
- 22 Macurek, L., Lindqvist, A., Lim, D., Lampson, M.A., Klompaker, R., Freire, R., et al. (2008) Polo-like kinase-1 is activated by aurora A to promote checkpoint recovery. *Nature* **455**, 119–123 <https://doi.org/doi:10.1038/nature07185>
- 23 Bucko, P.J., Lombard, C.K., Rathbun, L., Garcia, I., Bhat, A., Wordeman, L., et al. (2019) Subcellular drug targeting illuminates local kinase action. *eLife* **8**, e52220 <https://doi.org/doi:10.7554/eLife.52220>
- 24 Cunha-Ferreira, I., Bento, I., Pimenta-Marques, A., Jana, S.C., Lince-Faria, M., Duarte, P., et al. (2013) Regulation of autophosphorylation controls PLK4 self-destruction and centriole number. *Curr. Biol.* **23**, 2245–2254 <https://doi.org/doi:10.1016/j.cub.2013.09.037>
- 25 Sillibourne, J.E., Tack, F., Vloemans, N., Boeckx, A., Thambirajah, S., Bonnet, P., et al. (2010) Autophosphorylation of polo-like kinase 4 and its role in centriole duplication. *Mol. Biol. Cell* **21**, 547–561 <https://doi.org/doi:10.1091/mbc.e09-06-0505>
- 26 Shrestha, A., Hamilton, G., O'Neill, E., Knapp, S. and Elkins, J.M. (2012) Analysis of conditions affecting auto-phosphorylation of human kinases during expression in bacteria. *Protein Expr. Purif.* **81**, 136–143 <https://doi.org/doi:10.1016/j.pep.2011.09.012>
- 27 McSkimming, D.I., Dastgheib, S., Baffi, T.R., Byrne, D.P., Ferries, S., Scott, S.T., et al. (2016) KinView: a visual comparative sequence analysis tool for integrated kinome research. *Mol. Biosyst.* **12**, 3651–3665 <https://doi.org/doi:10.1039/C6MB00466K>
- 28 Leung, G.C., Hudson, J.W., Kozarova, A., Davidson, A., Dennis, J.W. and Sicheri, F. (2002) The Sak polo-box comprises a structural domain sufficient for mitotic subcellular localization. *Nat. Struct. Biol.* **9**, 719–724 <https://doi.org/doi:10.1038/nsb848>
- 29 Park, J.E., Zhang, L., Bang, J.K., Andresson, T., DiMaio, F. and Lee, K.S. (2019) Phase separation of Polo-like kinase 4 by autoactivation and clustering drives centriole biogenesis. *Nat. Commun.* **10**, 4959 <https://doi.org/doi:10.1038/s41467-019-12619-2>
- 30 Klebba, J.E., Buster, D.W., McLamarrah, T.A., Rusan, N.M. and Rogers, G.C. (2015) Autoinhibition and relief mechanism for Polo-like kinase 4. *Proc. Natl Acad. Sci. U.S.A.* **112**, E657–E666 <https://doi.org/doi:10.1073/pnas.1417967112>
- 31 Slevin, L.K., Nye, J., Pinkerton, D.C., Buster, D.W., Rogers, G.C. and Slep, K.C. (2012) The structure of the plk4 cryptic polo box reveals two tandem polo boxes required for centriole duplication. *Structure* **20**, 1905–1917 <https://doi.org/doi:10.1016/j.str.2012.08.025>
- 32 Arquint, C., Gabryjczyk, A.M., Imseng, S., Bohm, R., Sauer, E., Hiller, S., et al. (2015) STIL binding to Polo-box 3 of PLK4 regulates centriole duplication. *eLife* **4**, e07888 <https://doi.org/doi:10.7554/eLife.07888>
- 33 Zitouni, S., Nabais, C., Jana, S.C., Guerrero, A. and Bettencourt-Dias, M. (2014) Polo-like kinases: structural variations lead to multiple functions. *Nat. Rev. Mol. Cell Biol.* **15**, 433–452 <https://doi.org/doi:10.1038/nrm3819>
- 34 Cunha-Ferreira, I., Rodrigues-Martins, A., Bento, I., Riparbelli, M., Zhang, W., Laue, E., et al. (2009) The SCF/Slimb ubiquitin ligase limits centrosome amplification through degradation of SAK/PLK4. *Curr. Biol.* **19**, 43–49 <https://doi.org/doi:10.1016/j.cub.2008.11.037>
- 35 Kim, M., O'Rourke, B.P., Soni, R.K., Jallepalli, P.V., Hendrickson, R.C. and Tsou, M.B. (2016) Promotion and suppression of centriole duplication are catalytically coupled through PLK4 to ensure centriole homeostasis. *Cell Rep.* **16**, 1195–1203 <https://doi.org/doi:10.1016/j.celrep.2016.06.069>
- 36 Firat-Karalar, E.N., Rauniyar, N., Yates, III, J.R. and Stearns, T. (2014) Proximity interactions among centrosome components identify regulators of centriole duplication. *Curr. Biol.* **24**, 664–670 <https://doi.org/doi:10.1016/j.cub.2014.01.067>

- 37 Hatch, E.M., Kulukian, A., Holland, A.J., Cleveland, D.W. and Stearns, T. (2010) Cep152 interacts with Plk4 and is required for centriole duplication. *J. Cell Biol.* **191**, 721–729 <https://doi.org/doi:10.1083/jcb.201006049>
- 38 Denu, R.A., Sass, M.M., Johnson, J.M., Potts, G.K., Choudhary, A., Coon, J.J., et al. (2019) Polo-like kinase 4 maintains centriolar satellite integrity by phosphorylation of centrosomal protein 131 (CEP131). *J. Biol. Chem.* **294**, 6531–6549 <https://doi.org/doi:10.1074/jbc.RA118.004867>
- 39 Guderian, G., Westendorf, J., Uldschmid, A. and Nigg, E.A. (2010) Plk4 trans-autophosphorylation regulates centriole number by controlling betaTrCP-mediated degradation. *J. Cell Sci.* **123**, 2163–2169 <https://doi.org/doi:10.1242/jcs.068502>
- 40 Martin, C.A., Ahmad, I., Klingseisen, A., Hussain, M.S., Bicknell, L.S., Leitch, A., et al. (2014) Mutations in PLK4, encoding a master regulator of centriole biogenesis, cause microcephaly, growth failure and retinopathy. *Nat. Genet.* **46**, 1283–1292 <https://doi.org/doi:10.1038/ng.3122>
- 41 Takeda, Y., Kuroki, K., Chinen, T. and Kitagawa, D. (2020) Centrosomal and non-centrosomal functions emerged through eliminating centrosomes. *Cell Struct. Funct.* **45**, 57–64 <https://doi.org/doi:10.1247/csf.20007>
- 42 Nakajima, H., Toyoshima-Morimoto, F., Taniguchi, E. and Nishida, E. (2003) Identification of a consensus motif for Plk (Polo-like kinase) phosphorylation reveals Myt1 as a Plk1 substrate. *J. Biol. Chem.* **278**, 25277–25280 <https://doi.org/doi:10.1074/jbc.C300126200>
- 43 Garcia-Alvarez, B., de Carcer, G., Ibanez, S., Bragado-Nilsson, E. and Montoya, G. (2007) Molecular and structural basis of polo-like kinase 1 substrate recognition: Implications in centrosomal localization. *Proc. Natl Acad. Sci. U.S.A.* **104**, 3107–3112 <https://doi.org/doi:10.1073/pnas.0609131104>
- 44 Cozza, G. and Salvi, M. (2018) The Acidophilic Kinases PLK2 and PLK3: structure, Substrate Targeting and Inhibition. *Curr. Protein Pept. Sci.* **19**, 728–745 <https://doi.org/doi:10.2174/1389203719666180124095405>
- 45 Kettenbach, A.N., Wang, T., Faherty, B.K., Madden, D.R., Knapp, S., Bailey-Kellogg, C., et al. (2012) Rapid determination of multiple linear kinase substrate motifs by mass spectrometry. *Chem. Biol.* **19**, 608–618 <https://doi.org/doi:10.1016/j.chembiol.2012.04.011>
- 46 Johnson, E.F., Stewart, K.D., Woods, K.W., Giranda, V.L. and Luo, Y. (2007) Pharmacological and functional comparison of the polo-like kinase family: insight into inhibitor and substrate specificity. *Biochemistry* **46**, 9551–9563 <https://doi.org/doi:10.1021/bi7008745>
- 47 Leung, G.C., Ho, C.S., Blasutig, I.M., Murphy, J.M. and Sicheri, F. (2007) Determination of the Plk4/Sak consensus phosphorylation motif using peptide spots arrays. *FEBS Lett.* **581**, 77–83 <https://doi.org/doi:10.1016/j.febslet.2006.11.080>
- 48 Wong, Y.L., Anzola, J.V., Davis, R.L., Yoon, M., Motamedi, A., Kroll, A., et al. (2015) Cell biology. Reversible centriole depletion with an inhibitor of Polo-like kinase 4. *Science* **348**, 1155–1160 <https://doi.org/doi:10.1126/science.aaa5111>
- 49 Oegema, K., Davis, R.L., Lara-Gonzalez, P., Desai, A. and Shiau, A.K. (2018) CFI-400945 is not a selective cellular PLK4 inhibitor. *Proc. Natl Acad. Sci. U.S.A.* **115**, E10808–E10809 <https://doi.org/doi:10.1073/pnas.1813310115>
- 50 Tyler, R.K., Shpiro, N., Marquez, R. and Evers, P.A. (2007) VX-680 inhibits Aurora A and Aurora B kinase activity in human cells. *Cell Cycle* **6**, 2846–2854 <https://doi.org/doi:10.4161/cc.6.22.4940>
- 51 Bailey, F.P., Andreev, V.I. and Evers, P.A. (2014) The resistance tetrad: amino acid hotspots for kinome-wide exploitation of drug-resistant protein kinase alleles. *Methods Enzymol.* **548**, 117–146 <https://doi.org/doi:10.1016/B978-0-12-397918-6.00005-7>
- 52 Chinen, T., Yamamoto, S., Takeda, Y., Watanabe, K., Kuroki, K., Hashimoto, K., et al. (2020) NuMA assemblies organize microtubule asters to establish spindle bipolarity in acentrosomal human cells. *EMBO J.* **39**, e102378 <https://doi.org/doi:10.15252/embj.2019102378>
- 53 Ferrari, S., Marin, O., Pagano, M.A., Meggio, F., Hess, D., El-Shermely, M., et al. (2005) Aurora-A site specificity: a study with synthetic peptide substrates. *Biochem. J.* **390**, 293–302 <https://doi.org/doi:10.1042/BJ20050343>
- 54 Sardon, T., Pache, R.A., Stein, A., Molina, H., Vernos, I. and Aloy, P. (2010) Uncovering new substrates for Aurora A kinase. *EMBO Rep.* **11**, 977–984 <https://doi.org/doi:10.1038/embo.2010.171>
- 55 Sloane, D.A., Trkic, M.Z., Chu, M.L., Lamers, M.B., Mason, C.S., Mueller, I., et al. (2010) Drug-resistant aurora A mutants for cellular target validation of the small molecule kinase inhibitors MLN8054 and MLN8237. *ACS Chem. Biol.* **5**, 563–576 <https://doi.org/doi:10.1021/cb100053q>
- 56 Bury, L., Coelho, P.A., Simeone, A., Ferries, S., Evers, C.E., Evers, P.A., et al. (2017) Plk4 and Aurora A cooperate in the initiation of acentriolar spindle assembly in mammalian oocytes. *J. Cell Biol.* **216**, 3571–3590 <https://doi.org/doi:10.1083/jcb.201606077>
- 57 Scutt, P.J., Chu, M.L., Sloane, D.A., Cherry, M., Bignell, C.R., Williams, D.H., et al. (2009) Discovery and exploitation of inhibitor-resistant aurora and polo kinase mutants for the analysis of mitotic networks. *J. Biol. Chem.* **284**, 15880–15893 <https://doi.org/doi:10.1074/jbc.M109.005694>
- 58 Bozatz, P., Dingwell, K.S., Wu, K.Z., Cooper, F., Cummins, T.D., Hutchinson, L.D., et al. (2018) PAWS1 controls Wnt signalling through association with casein kinase 1alpha. *EMBO Rep.* **19**, e44807 <https://doi.org/doi:10.15252/embr.201744807>
- 59 Cosenza, M.R., Cazzola, A., Rossberg, A., Schieber, N.L., Konotop, G., Bausch, E., et al. (2017) Asymmetric centriole numbers at spindle poles cause chromosome missegregation in cancer. *Cell Rep.* **20**, 1906–1920 <https://doi.org/doi:10.1016/j.celrep.2017.08.005>
- 60 Ferries, S., Perkins, S., Brownridge, P.J., Campbell, A., Evers, P.A., Jones, A.R., et al. (2017) Evaluation of parameters for confident phosphorylation site localization using an orbitrap fusion tribrid mass spectrometer. *J. Proteome Res.* **16**, 3448–3459 <https://doi.org/doi:10.1021/acs.jproteome.7b00337>
- 61 Cox, J. and Mann, M. (2008) MaxQuant enables high peptide identification rates, individualized p.p.b.-range mass accuracies and proteome-wide protein quantification. *Nat. Biotechnol.* **26**, 1367–1372 <https://doi.org/doi:10.1038/nbt.1511>
- 62 Altschul, S.F., Gish, W., Miller, W., Myers, E.W. and Lipman, D.J. (1990) Basic local alignment search tool. *J. Mol. Biol.* **215**, 403–410 [https://doi.org/doi:10.1016/S0022-2836\(05\)80360-2](https://doi.org/doi:10.1016/S0022-2836(05)80360-2)
- 63 Edgar, R.C. (2004) MUSCLE: multiple sequence alignment with high accuracy and high throughput. *Nucleic Acids Res.* **32**, 1792–1797 <https://doi.org/doi:10.1093/nar/gkh340>
- 64 Desiere, F., Deutsch, E.W., King, N.L., Nesvizhskii, A.I., Mallick, P., Eng, J., et al. (2006) The PeptideAtlas project. *Nucleic Acids Res.* **34**, D655–D658 <https://doi.org/doi:10.1093/nar/gkj040>
- 65 Hornbeck, P.V., Zhang, B., Murray, B., Kornhauser, J.M., Latham, V. and Skrzypek, E. (2015) PhosphoSitePlus, 2014: mutations, PTMs and recalibrations. *Nucleic Acids Res.* **43**, D512–D520 <https://doi.org/doi:10.1093/nar/gku1267>
- 66 Colaert, N., Helsens, K., Martens, L., Vandekerckhove, J. and Gevaert, K. (2009) Improved visualization of protein consensus sequences by iceLogo. *Nat. Methods* **6**, 786–787 <https://doi.org/doi:10.1038/nmeth1109-786>
- 67 Huang da, W., Sherman, B.T. and Lempicki, R.A. (2009) Systematic and integrative analysis of large gene lists using DAVID bioinformatics resources. *Nat. Protoc.* **4**, 44–57 <https://doi.org/doi:10.1038/nprot.2008.211>
- 68 Huang da, W., Sherman, B.T. and Lempicki, R.A. (2009) Bioinformatics enrichment tools: paths toward the comprehensive functional analysis of large gene lists. *Nucleic Acids Res.* **37**, 1–13 <https://doi.org/doi:10.1093/nar/gkn923>

- 69 Szklarczyk, D., Franceschini, A., Wyder, S., Forslund, K., Heller, D., Huerta-Cepas, J., et al. (2015) STRING v10: protein-protein interaction networks, integrated over the tree of life. *Nucleic Acids Res.* **43**, D447–D452 <https://doi.org/doi:10.1093/nar/gku1003>
- 70 Byrne, D.P., Vonderach, M., Ferries, S., Brownridge, P.J., Evers, C.E. and Evers, P.A. (2016) cAMP-dependent protein kinase (PKA) complexes probed by complementary differential scanning fluorimetry and ion mobility-mass spectrometry. *Biochem. J.* **473**, 3159–3175 <https://doi.org/doi:10.1042/BCJ20160648>
- 71 Byrne, D.P., Li, Y., Ngamlert, P., Ramakrishnan, K., Evers, C.E., Wells, C., et al. (2018) New tools for evaluating protein tyrosine sulfation: tyrosylprotein sulfotransferases (TPSTs) are novel targets for RAF protein kinase inhibitors. *Biochem. J.* **475**, 2435–2455 <https://doi.org/doi:10.1042/BCJ20180266>
- 72 Caron, D., Byrne, D.P., Thebault, P., Soulet, D., Landry, C.R., Evers, P.A., et al. (2016) Mitotic phosphotyrosine network analysis reveals that tyrosine phosphorylation regulates Polo-like kinase 1 (PLK1). *Sci. Signal.* **9**, rs14 <https://doi.org/doi:10.1126/scisignal.aah3525>
- 73 Wilson, L.J., Linley, A., Hammond, D.E., Hood, F.E., Coulson, J.M., MacEwan, D.J., et al. (2018) New Perspectives, Opportunities, and Challenges in Exploring the Human Protein Kinome. *Cancer Res.* **78**, 15–29 <https://doi.org/doi:10.1158/0008-5472.CAN-17-2291>
- 74 Bain, J., Plater, L., Elliott, M., Shpiro, N., Hastie, C.J., McLauchlan, H., et al. (2007) The selectivity of protein kinase inhibitors: a further update. *Biochem. J.* **408**, 297–315 <https://doi.org/doi:10.1042/BJ20070797>
- 75 Grosstessner-Hain, K., Hegemann, B., Novatchkova, M., Rameseder, J., Joughin, B.A., Hudecz, O., et al. (2011) Quantitative phospho-proteomics to investigate the polo-like kinase 1-dependent phospho-proteome. *Mol. Cell Proteomics* **10**, M111 008540 <https://doi.org/doi:10.1074/mcp.M111.008540>
- 76 Kettenbach, A.N., Schweppe, D.K., Faherty, B.K., Pechenick, D., Pletnev, A.A. and Gerber, S.A. (2011) Quantitative phosphoproteomics identifies substrates and functional modules of Aurora and Polo-like kinase activities in mitotic cells. *Sci. Signal.* **4**, rs5 <https://doi.org/doi:10.1126/scisignal.2001497>
- 77 Ong, S.E., Kratchmarova, I. and Mann, M. (2003) Properties of ¹³C-substituted arginine in stable isotope labeling by amino acids in cell culture (SILAC). *J. Proteome Res.* **2**, 173–181 <https://doi.org/doi:10.1021/pr0255708>
- 78 Oppermann, F.S., Gnad, F., Olsen, J.V., Hornberger, R., Greff, Z., Kerl, G., et al. (2009) Large-scale proteomics analysis of the human kinome. *Mol. Cell Proteomics* **8**, 1751–1764 <https://doi.org/doi:10.1074/mcp.M800588-MCP200>
- 79 Sonnen, K.F., Gabryjczyk, A.M., Anselm, E., Stierhof, Y.D. and Nigg, E.A. (2013) Human Cep192 and Cep152 cooperate in Plk4 recruitment and centriole duplication. *J. Cell Sci.* **126**, 3223–3233 <https://doi.org/doi:10.1242/jcs.129502>
- 80 Cizmecioglu, O., Arnold, M., Bahtz, R., Settele, F., Ehret, L., Haselmann-Weiss, U., et al. (2010) Cep152 acts as a scaffold for recruitment of Plk4 and CPAP to the centrosome. *J. Cell Biol.* **191**, 731–739 <https://doi.org/doi:10.1083/jcb.201007107>
- 81 Dzhindzhev, N.S., Yu, Q.D., Weiskopf, K., Tzolovsky, G., Cunha-Ferreira, I., Riparbelli, M., et al. (2010) Asterless is a scaffold for the onset of centriole assembly. *Nature* **467**, 714–718 <https://doi.org/doi:10.1038/nature09445>
- 82 Xu, X., Huang, S., Zhang, B., Huang, F., Chi, W., Fu, J., et al. (2017) DNA replication licensing factor Cdc6 and Plk4 kinase antagonistically regulate centrosome duplication via Sas-6. *Nat. Commun.* **8**, 15164 <https://doi.org/doi:10.1038/ncomms15164>
- 83 Arquint, C., Cubizolles, F., Morand, A., Schmidt, A. and Nigg, E.A. (2018) The SKP1-Cullin-F-box E3 ligase betaTrCP and CDK2 cooperate to control STIL abundance and centriole number. *Open Biol.* **8**, 170253 <https://doi.org/doi:10.1098/rsob.170253>
- 84 Zitouni, S., Francia, M.E., Leal, F., Montenegro Gouveia, S., Nabais, C., Duarte, P., et al. (2016) CDK1 Prevents Unscheduled PLK4-STIL Complex Assembly in Centriole Biogenesis. *Curr. Biol.* **26**, 1127–1137 <https://doi.org/doi:10.1016/j.cub.2016.03.055>
- 85 Zheng, Y., Yang, W., Xia, Y., Hawke, D., Liu, D.X. and Lu, Z. (2011) Ras-induced and extracellular signal-regulated kinase 1 and 2 phosphorylation-dependent isomerization of protein tyrosine phosphatase (PTP)-PEST by PIN1 promotes FAK dephosphorylation by PTP-PEST. *Mol. Cell Biol.* **31**, 4258–4269 <https://doi.org/doi:10.1128/MCB.05547-11>
- 86 Sjostrom, S.K., Finn, G., Hahn, W.C., Rowitch, D.H. and Kenney, A.M. (2005) The Cdk1 complex plays a prime role in regulating N-myc phosphorylation and turnover in neural precursors. *Dev. Cell* **9**, 327–338 <https://doi.org/doi:10.1016/j.devcel.2005.07.014>
- 87 Richards, M.W., Burgess, S.G., Poon, E., Carstensen, A., Eilers, M., Chesler, L., et al. (2016) Structural basis of N-Myc binding by Aurora-A and its destabilization by kinase inhibitors. *Proc. Natl Acad. Sci. U.S.A.* **113**, 13726–13731 <https://doi.org/doi:10.1073/pnas.1610626113>
- 88 Yada, M., Hatakeyama, S., Kamura, T., Nishiyama, M., Tsunematsu, R., Imaki, H., et al. (2004) Phosphorylation-dependent degradation of c-Myc is mediated by the F-box protein Fbw7. *EMBO J.* **23**, 2116–2125 <https://doi.org/doi:10.1038/sj.emboj.7600217>
- 89 Otto, T., Horn, S., Brockmann, M., Eilers, U., Schuttrumpf, L., Popov, N., et al. (2009) Stabilization of N-Myc is a critical function of Aurora A in human neuroblastoma. *Cancer Cell* **15**, 67–78 <https://doi.org/doi:10.1016/j.ccr.2008.12.005>
- 90 Tollenaere, M.A.X., Villumsen, B.H., Blasius, M., Nielsen, J.C., Wagner, S.A., Bartek, J., et al. (2015) p38- and MK2-dependent signalling promotes stress-induced centriolar satellite remodelling via 14-3-3-dependent sequestration of CEP131/AZI1. *Nat. Commun.* **6**, 10075 <https://doi.org/doi:10.1038/ncomms10075>
- 91 Barone, G., Staples, C.J., Ganesh, A., Patterson, K.W., Bryne, D.P., Myers, K.N., et al. (2016) Human CDK18 promotes replication stress signaling and genome stability. *Nucleic Acids Res.* **44**, 8772–8785 <https://doi.org/doi:10.1093/nar/gkw615>
- 92 Petrinac, S., Ganuelas, M.L., Bonni, S., Nantais, J. and Hudson, J.W. (2009) Polo-like kinase 4 phosphorylates Chk2. *Cell Cycle* **8**, 327–329 <https://doi.org/doi:10.4161/cc.8.2.7355>
- 93 O'Neill, T., Giarratani, L., Chen, P., Iyer, L., Lee, C.H., Bobiak, M., et al. (2002) Determination of substrate motifs for human Chk1 and hCds1/Chk2 by the oriented peptide library approach. *J. Biol. Chem.* **277**, 16102–16115 <https://doi.org/doi:10.1074/jbc.M111705200>
- 94 Brown, N.R., Noble, M.E., Lawrie, A.M., Morris, M.C., Tunnah, P., Divita, G., et al. (1999) Effects of phosphorylation of threonine 160 on cyclin-dependent kinase 2 structure and activity. *J. Biol. Chem.* **274**, 8746–8756 <https://doi.org/doi:10.1074/jbc.274.13.8746>
- 95 Jeffrey, P.D., Russo, A.A., Polyak, K., Gibbs, E., Hurwitz, J., Massague, J., et al. (1995) Mechanism of CDK activation revealed by the structure of a cyclinA-CDK2 complex. *Nature* **376**, 313–320 <https://doi.org/doi:10.1038/376313a0>
- 96 De Bondt, H.L., Rosenblatt, J., Jancarik, J., Jones, H.D., Morgan, D.O. and Kim, S.H. (1993) Crystal structure of cyclin-dependent kinase 2. *Nature* **363**, 595–602 <https://doi.org/doi:10.1038/363595a0>
- 97 Echallier, A., Endicott, J.A. and Noble, M.E. (2010) Recent developments in cyclin-dependent kinase biochemical and structural studies. *Biochim. Biophys. Acta* **1804**, 511–519 <https://doi.org/doi:10.1016/j.bbapap.2009.10.002>

- 98 Suzuki, K., Sako, K., Akiyama, K., Isoda, M., Senoo, C., Nakajo, N., et al. (2015) Identification of non-Ser/Thr-Pro consensus motifs for Cdk1 and their roles in mitotic regulation of C2H2 zinc finger proteins and Ect2. *Sci. Rep.* **5**, 7929 <https://doi.org/doi:10.1038/srep07929>
- 99 Ord, M., Moll, K., Agerova, A., Kivi, R., Faustova, I., Venta, R., et al. (2019) Multisite phosphorylation code of CDK. *Nat. Struct. Mol. Biol.* **26**, 649–658 <https://doi.org/doi:10.1038/s41594-019-0256-4>
- 100 Basu, S., Roberts, E.L., Jones, A.W., Swaffer, M.P., Snijders, A.P. and Nurse, P. (2020) The hydrophobic patch directs cyclin B to centrosomes to promote global CDK phosphorylation at mitosis. *Curr. Biol.* **30**, 883–892 e4 <https://doi.org/doi:10.1016/j.cub.2019.12.053>
- 101 Swaffer, M.P., Jones, A.W., Flynn, H.R., Snijders, A.P. and Nurse, P. (2016) CDK substrate phosphorylation and ordering the cell cycle. *Cell* **167**, 1750–1761 e16 <https://doi.org/doi:10.1016/j.cell.2016.11.034>
- 102 Kelly, J.R., Martini, S., Brownlow, N., Joshi, D., Federico, S., Jamshidi, S., et al. (2020) The Aurora B specificity switch is required to protect from non-disjunction at the metaphase/anaphase transition. *Nat. Commun.* **11**, 1396 <https://doi.org/doi:10.1038/s41467-020-15163-6>
- 103 Perez-Riverol, Y., Csordas, A., Bai, J., Bernal-Llinares, M., Hewapathirana, S., Kundu, D.J., et al. (2019) The PRIDE database and related tools and resources in 2019: improving support for quantification data. *Nucleic Acids Res.* **47**, D442–D450 <https://doi.org/doi:10.1093/nar/gky1106>